

Supporting Information

Crown ether-appended calix[2]triazolium[2]arene as a
macrocyclic receptor for the recognition of the H_2PO_4^-
anion

Jihee Cho,^{‡a} Peter Verwilt,^{‡b} Minjung Kang,^b Jia-Lin Pan,^b Amit Sharma,^b Chang Seop
Hong,^{*b} Jong Seung Kim^{*b} and Sanghee Kim^{*a}

^a College of Pharmacy, Seoul National University, 1 Gwanak-ro, Gwanak-gu, Seoul, 08826,
Korea

^b Department of Chemistry, Korea University, Seoul 02841, Korea

[‡] equally contributed

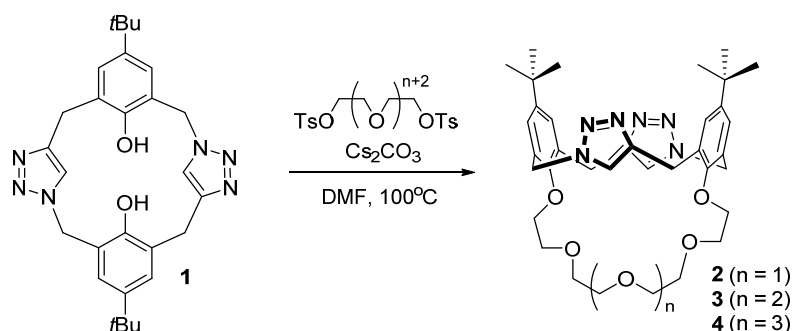
Contents

1. Synthesis	S1–S6
2. X-Ray Crystallographic Data	S7–S13
3. NOESY spectral analysis	S14–S16
4. Details of NMR spectroscopic binding studies	S17–S25
5. Titration experiment	S26–S33
6. Detection limit measurements	S34
7. Theoretical studies	S35
8. Simulated ¹H NMR spectra	S36
9. NMR Spectra	S37–S44
10. References	S45

1. Synthesis

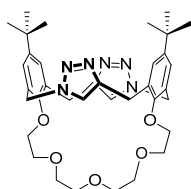
General methods. All of the chemicals were reagent grade and used as purchased. All of the reactions were performed under an inert atmosphere of dry nitrogen using distilled dry solvents. The reaction progress was monitored by thin layer chromatography (TLC) analysis using silica gel 60 F-254 TLC plates. The compound spots were visualized using UV light. Melting points were measured using a Buchi B-540 melting point apparatus without correction. Flash column chromatography was carried out on silica gel (230–400 mesh). ^1H and ^{13}C NMR spectra were recorded on Bruker Avance-500 (500MHz) or Jeol JNM-ECA-600 (600MHz) spectrometer at 278K. Chemical shifts are reported in ppm (δ) units relative to the undeuterated solvent as a reference peak ($\text{CD}_3\text{CN}-d_3$: 1.94 ppm/ ^1H NMR, 1.32 and 118.26 ppm/ ^{13}C NMR). The following abbreviations are used to represent NMR peak multiplicities: s (singlet), d (doublet), t (triplet), m (multiplet) and br (broad). IR spectra were measured by an Agilent Technologies 5500 Series FT-IR spectrometer. High-resolution mass spectra (HRMS) were recorded using Fast atom bombardment (FAB) mass spectroscopy.

General procedure of synthesis of crown ether containing calix[2]triazole[2]arene (2–4).



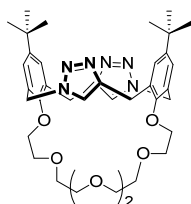
The crown ether containing calix[2]triazole[2]arenes **2–4** were prepared from the calix[2]triazole[2]arene **1** and corresponding ethylene glycol ditosylate. Cs₂CO₃ (1.85 mmol, 6 equiv) was added to a solution of calix[2]triazole[2]arene **1** (0.308 mmol, 1 equiv) and the corresponding ethylene glycol ditosylate (0.370 mmol, 1.2 equiv) in anhydrous DMF (31 mL) under a nitrogen atmosphere. After heating at 100°C for 3 days, the reaction mixture was cooled to room temperature.

DMF was removed *in vacuo* and the crude product was purified by column chromatography on silica gel using CH₂Cl₂/methanol mixtures as the eluent.



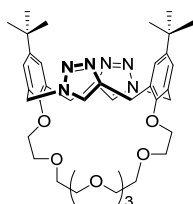
Crown ether containing calix[2]triazole[2]arene (2)

Following the general procedure, the crude product was purified using column chromatography on silica gel (CH₂Cl₂/methanol, 20:1 *v/v*) to yield product **2** (185 mg, 93%) as a white solid; m.p. 258–262 °C; ¹H NMR (CD₃CN, 500 MHz) δ 7.97 (s, 2H), 7.25 (s, 4H), 5.73 (d, *J* = 13.7 Hz, 2H), 5.17 (d, *J* = 13.7 Hz, 2H), 4.30 (d, *J* = 14.1 Hz, 2H), 4.22–4.18 (m, 2H), 4.05–4.00 (m, 2H), 3.99–3.95 (m, 4H), 3.74–3.72 (m, 4H), 3.64 (d, *J* = 14.2 Hz, 2H), 3.62–3.60 (m, 4H), 1.15 (s, 18H) ppm.; ¹³C NMR (CD₃CN, 125 MHz) δ 154.2 (2C), 148.8 (2C), 148.0 (2C), 135.8 (2C), 130.8 (2C), 129.5 (2C), 127.9 (2C), 123.2 (2C), 75.0 (2C), 71.8 (2C), 71.1 (4C), 50.6 (2C), 34.9 (2C), 31.4 (6C), 29.4 (2C) ppm.; IR (CH₂Cl₂) ν_{max} 2953, 2904, 2866, 1483, 1200, 1111, 1047, 935, 733 (cm⁻¹); HRMS (FAB) *m/z* calcd for C₃₆H₄₉N₆O₅ 645.3764 ([M+H]⁺), found 645.3756.



Crown ether containing calix[2]triazole[2]arene (3)

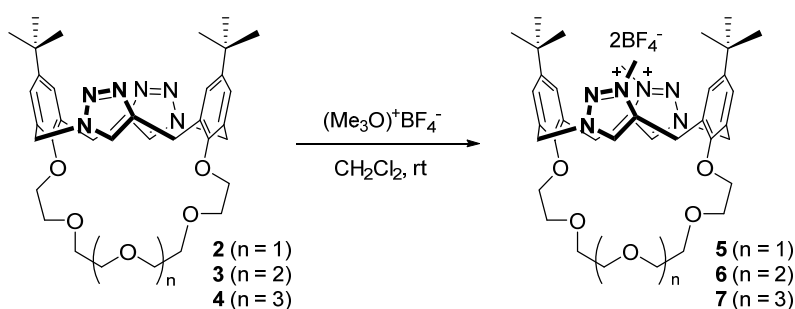
Following the general procedure, the crude product was purified using column chromatography on silica gel (CH₂Cl₂/methanol, 20:1 *v/v*) to yield product **3** (166 mg, 78%) as a white solid; m.p. 218–221 °C; ¹H NMR (CD₃CN, 600 MHz) δ 7.88 (s, 2H), 7.27 (s, 4H), 5.72 (d, *J* = 14.2 Hz, 2H), 5.18 (d, *J* = 13.8 Hz, 2H), 4.27–4.22 (m, 4H), 4.10–4.07 (m, 2H), 3.95–3.87 (m, 4H), 3.71–3.66 (m, 6H), 3.65–3.60 (m, 4H), 3.47 (s, 4H), 1.16 (s, 18H) ppm.; ¹³C NMR (CD₃CN, 150 MHz) δ 154.1 (2C), 148.7 (2C), 147.9 (2C), 135.6 (2C), 130.7 (2C), 129.6 (2C), 128.0 (2C), 123.2 (2C), 74.5 (2C), 71.4 (2C), 71.3 (2C), 71.2 (2C), 71.1 (2C), 50.8 (2C), 34.9 (2C), 31.4 (6C), 29.5 (2C) ppm.; IR (CH₂Cl₂) ν_{max} 2951, 2864, 1483, 1362, 1201, 1111, 1045, 928, 732 (cm⁻¹); HRMS (FAB) *m/z* calcd for C₃₈H₅₃N₆O₆ 689.4027 ([M+H]⁺), found 689.4031.



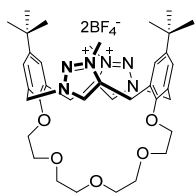
Crown ether containing calix[2]triazole[2]arene (**4**)

Following the general procedure, the crude product was purified using column chromatography on silica gel ($\text{CH}_2\text{Cl}_2/\text{methanol}$, 20:1 *v/v*) to yield product **4** (206 mg, 91%) as a white solid; m.p. 180–184 °C; ^1H NMR (CD_3CN , 500 MHz) δ 7.92 (s, 2H), 7.26 (s, 4H), 5.74 (d, $J = 13.8$ Hz, 2H), 5.17 (d, $J = 13.9$ Hz, 2H), 4.28 (d, $J = 14.2$ Hz, 2H), 4.26–4.24 (m, 2H), 4.11–4.08 (m, 2H), 3.94–3.87 (m, 4H), 3.69–3.67 (m, 5H), 3.65–3.61 (m, 5H), 3.51–3.48 (m, 4H), 3.37–3.36 (m, 4H), 1.16 (s, 18H) ppm.; ^{13}C NMR (CD_3CN , 125 MHz) δ 154.0 (2C), 148.7 (2C), 148.0 (2C), 135.7 (2C), 130.7 (2C), 129.6 (2C), 127.9 (2C), 123.3 (2C), 74.3 (2C), 71.41 (4C), 71.39 (2C), 71.1 (2C), 71.0 (2C), 50.8 (2C), 34.9 (2C), 31.4 (6C), 29.5 (2C) ppm; IR (CH_2Cl_2) ν_{max} 2954, 2904, 2868, 1675, 1484, 1364, 1203, 1112, 1047, 734 (cm^{-1}); HRMS (FAB) m/z calcd for $\text{C}_{40}\text{H}_{57}\text{N}_6\text{O}_7$ 733.4289 ($[\text{M}+\text{H}]^+$), found 733.4295.

General procedure of synthesis of crown ether containing calix[2]triazolium[2]arene (**5–7**).

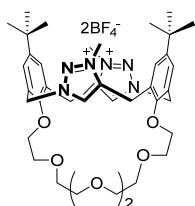


The crown ether containing calix[2]triazolium[2]arene **5–7** were prepared from the corresponding crown ether containing calix[2]triazole[2]arene **2–4**. $(\text{Me}_3\text{O})^+\text{BF}_4^-$ (0.810 mmol, 3 equiv) was added to a solution of crown ether containing calix[2]triazole[2]arene **2–4** (0.270 mmol, 1 equiv) in CH_2Cl_2 (108 mL) under nitrogen atmosphere. The reaction mixture was stirred at room temperature for 12 h. Thereafter, methanol (4.50 mL) was added to quench the reaction, and then the solution concentrated *in vacuo*. The crude product was purified by column chromatography on silica gel using $\text{CH}_2\text{Cl}_2/\text{methanol}/\text{AcOH}$ mixtures as the eluent.



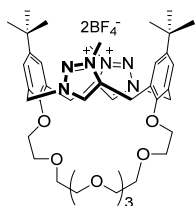
Crown ether containing calix[2]triazolium[2]arene (**5**)

Following the general procedure, the crude product was purified using column chromatography on silica gel (CH₂Cl₂/methanol, 20:1 v/v, 1% AcOH) to yield product **5** (176 mg, 77%) as a white solid; m.p. 110–120 °C; ¹H NMR (CD₃CN, 500 MHz) δ 8.14 (s, 2H), 7.46 (d, *J* = 2.3 Hz, 2H), 7.42 (d, *J* = 2.3 Hz, 2H), 6.08 (d, *J* = 14.1 Hz, 2H), 5.34 (d, *J* = 14.2 Hz, 2H), 4.57 (d, *J* = 15.9 Hz, 2H), 4.18–4.14 (m, 2H), 4.09–4.06 (m, 8H), 3.89–3.81 (m, 6H), 3.78–3.71 (m, 4H), 3.62 (t, *J* = 4.2 Hz, 4H), 1.20 (s, 18H) ppm.; ¹³C NMR (CD₃CN, 125 MHz) δ 154.9 (2C), 149.8 (2C), 143.3 (2C), 131.3 (2C), 130.1 (2C), 129.9 (2C), 129.8 (2C), 127.4 (2C), 75.7 (2C), 70.7 (2C), 70.5 (2C), 70.1 (2C), 54.1 (2C), 38.5 (2C), 35.1 (2C), 31.3 (6C), 26.2 (2C) ppm.; IR (CH₂Cl₂) ν_{max} 2958, 2871, 1574, 1489, 1365, 1205, 1048, 932, 734 (cm⁻¹); HRMS (FAB) *m/z* calcd for C₃₈H₅₄BF₄N₆O₅ 761.4192 ([M–BF₄]⁺), found 761.4197.



Crown ether containing calix[2]triazolium[2]arene (**6**)

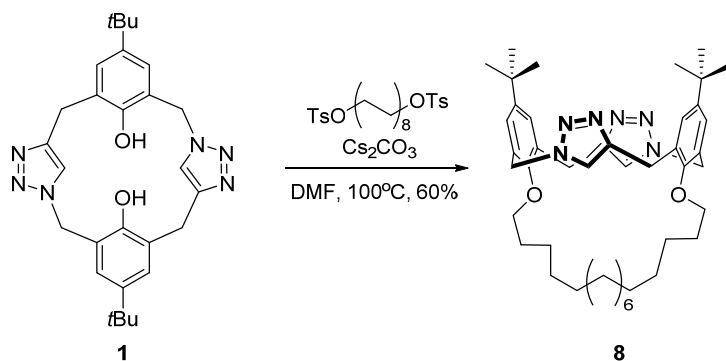
Following the general procedure, the crude product was purified using column chromatography on silica gel (CH₂Cl₂/methanol, 20:1 v/v, 1% AcOH) to yield product **6** (154 mg, 64%) as a white solid; m.p. 160–165 °C; ¹H NMR (CD₃CN, 500 MHz) δ 8.11 (s, 2H), 7.44 (d, *J* = 2.0 Hz, 2H), 7.41 (d, *J* = 2.1 Hz, 2H), 6.05 (d, *J* = 14.3 Hz, 2H), 5.32 (d, *J* = 14.3 Hz, 2H), 4.50 (d, *J* = 16.0 Hz, 2H), 4.24–4.20 (m, 2H), 4.13–4.08 (m, 8H), 3.87–3.79 (m, 6H), 3.69–3.67 (m, 4H), 3.66–3.58 (m, 4H), 3.44 (s, 4H), 1.20 (s, 18H) ppm.; ¹³C NMR (CD₃CN, 125 MHz) δ 154.7 (2C), 149.7 (2C), 143.0 (2C), 131.4 (2C), 130.1 (2C), 130.0 (2C), 129.7 (2C), 127.4 (2C), 74.9 (2C), 71.2 (2C), 70.6 (2C), 70.5 (2C), 70.2 (2C), 54.3 (2C), 38.4 (2C), 35.1 (2C), 31.3 (6C), 26.3 (2C) ppm.; IR (CH₂Cl₂) ν_{max} 2957, 2871, 1576, 1490, 1366, 1207, 1057, 1036, 932, 734 (cm⁻¹); HRMS (FAB) *m/z* calcd for C₄₀H₅₈BF₄N₆O₆ 805.4454 ([M]⁺), found 805.4444.



Crown ether containing calix[2]triazolium[2]arene (**7**)

Following the general procedure, the crude product was purified using column chromatography on silica gel (CH₂Cl₂/methanol, 20:1 v/v, 1% AcOH) to yield product **7** (220 mg, 86%) as a white solid; m.p. 195–200 °C; ¹H NMR (CD₃CN, 500 MHz) δ 8.18 (s, 2H), 7.46 (d, *J* = 2.3 Hz, 2H), 7.42 (d, *J* = 2.3 Hz, 2H), 6.08 (d, *J* = 14.4 Hz, 2H), 5.34 (d, *J* = 14.3 Hz, 2H), 4.57 (d, *J* = 16.0 Hz, 2H), 4.23 (dt, *J* = 11.5, 3.9 Hz, 2H), 4.13 (dt, *J* = 11.5, 3.9 Hz, 2H), 4.09 (s, 6H), 3.85–3.82 (m, 6H), 3.72–3.66 (m, 4H), 3.65–3.57 (m, 4H), 3.53–3.46 (m, 4H), 3.36–3.29 (m, 4H), 1.21 (s, 18H) ppm.; ¹³C NMR (CD₃CN, 125 MHz) δ 154.6 (2C), 149.7 (2C), 143.1 (2C), 131.3 (2C), 130.2 (2C), 130.1 (2C), 129.9 (2C), 127.5 (2C), 74.7 (2C), 71.4 (2C), 71.0 (2C), 70.6 (4C), 70.4 (2C), 54.4 (2C), 38.4 (2C), 35.1 (2C), 31.3 (6C), 26.3 (2C) ppm; IR (CH₂Cl₂) ν_{max} 2956, 2905, 2872, 1575, 1490, 1366, 1206, 1052, 1036, 732 (cm⁻¹); HRMS (FAB) *m/z* calcd for C₄₂H₆₂BF₄N₆O₇ 849.4716 ([M–BF₄⁻]⁺), found 849.4697.

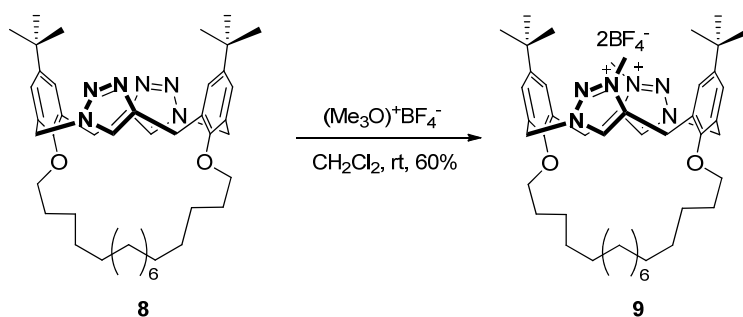
Synthesis of alkyl chain containing calix[2]triazole[2]arene (**8**).



Cs₂CO₃ (603 mg, 1.85 mmol) was added to a solution of calix[2]triazole[2]arene **1** (150 mg, 0.308 mmol) and ditosylate^{S1} (210 mg, 0.370 mmol) in anhydrous DMF (31 mL) under a nitrogen atmosphere. After heating at 100°C for 3 days and then allowing to cool, the DMF was removed *in vacuo*. The crude product was purified using column chromatography on silica gel (CH₂Cl₂/methanol, 20:1 v/v) to yield product **8** (131 mg, 60%) as a white solid; m.p. 108–113 °C; ¹H NMR (CD₃CN, 500 MHz) δ 7.84 (s, 2H), 7.25 (s, 4H), 5.49 (d, *J* = 13.9 Hz, 2H), 5.22 (d, *J* = 13.9 Hz, 2H), 4.15 (d, *J* = 14.3 Hz, 2H), 3.99

(dd, $J = 16.4, 8.4$ Hz, 2H), 3.92 (dd, $J = 15.1, 7.5$ Hz, 2H), 3.69 (d, $J = 14.3$ Hz, 2H), 1.99 (t, $J = 7.05$ Hz, 4H), 1.42–1.33 (m, 20H), 1.25 (t, $J = 9.05$ Hz, 4H), 1.14 (s, 18H) ppm.; ^{13}C NMR (CD_3CN , 125 MHz) δ 154.1 (2C), 148.8 (2C), 148.3 (2C), 135.6 (2C), 130.4 (2C), 129.7 (2C), 128.0 (2C), 122.7 (2C), 75.4 (2C), 51.0 (2C), 34.9 (2C), 31.7 (2C), 31.4 (6C), 29.6 (2C), 29.4 (2C), 28.9 (2C), 27.9 (2C), 26.7 (2C), 26.3 (2C), 26.1 (2C) ppm; IR (CH_2Cl_2) ν_{max} 2926, 2853, 1479, 1363, 1203, 1106, 1046, 992, 733 (cm^{-1}); HRMS (FAB) m/z calcd for $\text{C}_{44}\text{H}_{65}\text{N}_6\text{O}_2$ 709.5169 ($[\text{M}+\text{H}]^+$), found 709.5168.

Synthesis of alkyl chain containing calix[2]triazolium[2]arene (**9**).



$(\text{Me}_3\text{O})^+\text{BF}_4^-$ (125 mg, 0.846 mmol) was added to a solution of triazole **8** (200 mg, 0.282 mmol) in CH_2Cl_2 (113 mL) under nitrogen atmosphere. The reaction mixture was stirred at room temperature for 12 h and methanol (4.70 mL) was added to quench the reaction, and then the solution was concentrated *in vacuo*. The crude product was purified using column chromatography on silica gel (CH_2Cl_2 /methanol, 20:1 *v/v*, 1% AcOH) to yield product **9** (154 mg, 60%) as a white solid; m.p. 123–128 °C; ^1H NMR (CD_3CN , 500 MHz) δ 7.66 (s, 2H), 7.46 (d, $J = 2.2$ Hz, 2H), 7.44 (d, $J = 2.2$ Hz, 2H), 5.76 (d, $J = 14.7$ Hz, 2H), 5.40 (d, $J = 14.7$ Hz, 2H), 4.27 (d, $J = 16.4$ Hz, 2H), 4.19 (s, 6H), 3.90–3.85 (m, 6H), 1.79–1.73 (m, 4H), 1.34–1.23 (m, 24H), 1.20 (s, 18H) ppm.; ^{13}C NMR (CD_3CN , 150 MHz) δ 154.5 (2C), 149.9 (2C), 144.3 (2C), 131.8 (2C), 130.6 (2C), 129.7 (2C), 128.7 (2C), 126.3 (2C), 75.7 (2C), 54.9 (2C), 38.6 (2C), 35.2 (2C), 31.5 (2C), 31.3 (6C), 29.5 (2C), 29.0 (2C), 27.9 (2C), 26.7 (2C), 26.6 (2C), 26.1 (2C), 26.0 (2C) ppm; IR (CH_2Cl_2) ν_{max} 2928, 2857, 1577, 1491, 1367, 1208, 1055, 984, 732 (cm^{-1}); HRMS (FAB) m/z calcd for $\text{C}_{46}\text{H}_{70}\text{BF}_4\text{N}_6\text{O}_2$ 825.5597 ($[\text{M}-\text{BF}_4]^-$), found 825.5593.

2. X-Ray Crystallographic Data

X-ray crystallographic data for 2

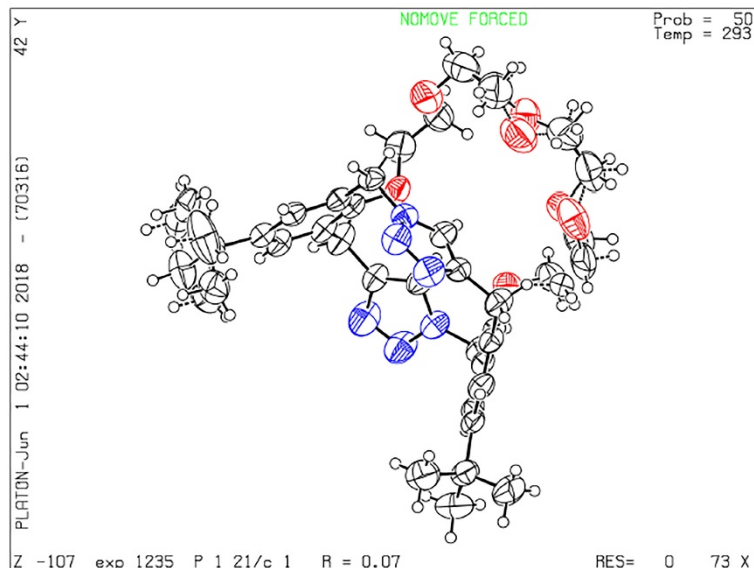


Figure S1. X-ray crystal structure of **2**. CCDC 1916779 (**2**) contains the supplementary crystallographic data for this paper. These data can be obtained free of charge from the Cambridge Crystallographic Data Centre via www.ccdc.cam.ac.uk/data_request/cif.

Table S1. Crystal data and structure refinement for **2**.

Empirical formula	C ₃₆ H ₄₈ N ₆ O ₅
Formula weight	644.80
Temperature/K	292.8(3)
Crystal system	monoclinic
Space group	P2 ₁ /c
a/Å	10.4230(3)
b/Å	20.3482(7)
c/Å	17.1498(7)
α/°	90
β/°	106.795(4)
γ/°	90
Volume/Å ³	3482.1(2)
Z	4
ρ _{calc} /cm ³	1.230
μ/mm ⁻¹	0.669
F(000)	1384.0

Crystal size/mm ³	0.436 × 0.311 × 0.155
Radiation	CuKα (λ = 1.54184)
2θ range for data collection/°	6.918 to 147.4
Index ranges	-12 ≤ h ≤ 8, -24 ≤ k ≤ 23, -20 ≤ l ≤ 20
Reflections collected	13883
Independent reflections	6803 [R _{int} = 0.0324, R _{sigma} = 0.0391]
Data/restraints/parameters	6803/0/497
Goodness-of-fit on F ²	1.025
Final R indexes [I >= 2σ (I)]	R ₁ = 0.0728, wR ₂ = 0.2120
Final R indexes [all data]	R ₁ = 0.0901, wR ₂ = 0.2348
Largest diff. peak/hole / e Å ⁻³	0.44/-0.34

X-ray crystallographic data for 3

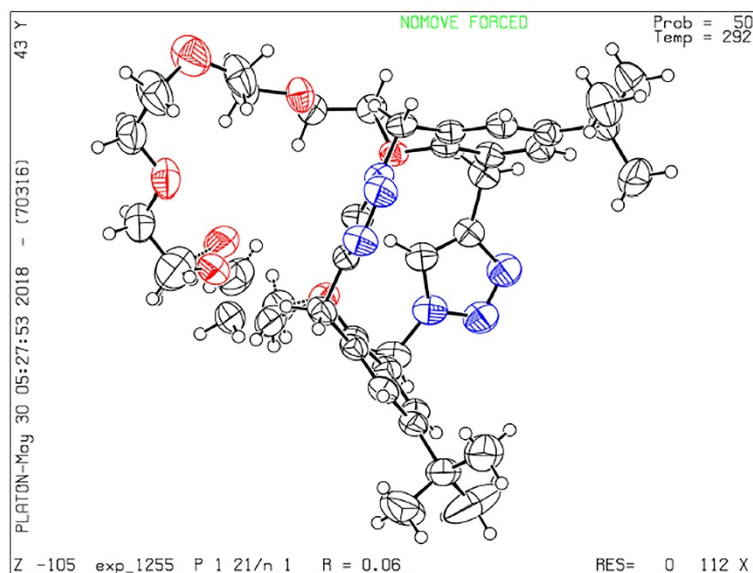


Figure S2. X-ray crystal structure of **3**. CCDC 1916782 (**3**) contains the supplementary crystallographic data for this paper. These data can be obtained free of charge from the Cambridge Crystallographic Data Centre via www.ccdc.cam.ac.uk/data_request/cif.

Table S2. Crystal data and structure refinement for **3**.

Empirical formula	C ₃₈ H ₅₂ N ₆ O ₆
Formula weight	688.85
Temperature/K	292(3)
Crystal system	monoclinic
Space group	P2 ₁ /n
a/Å	10.4036(2)
b/Å	19.8880(4)
c/Å	18.5228(4)
α/°	90
β/°	103.284(2)
γ/°	90
Volume/Å ³	3729.95(13)
Z	4
ρ _{calc} /cm ³	1.227
μ/mm ⁻¹	0.677
F(000)	1480.0
Crystal size/mm ³	0.685 × 0.462 × 0.344
Radiation	CuKα (λ = 1.54184)
2θ range for data collection/°	6.618 to 147.842
Index ranges	-12 ≤ h ≤ 12, -24 ≤ k ≤ 24, -23 ≤ l ≤ 22
Reflections collected	28406
Independent reflections	7434 [R _{int} = 0.0296, R _{sigma} = 0.0216]
Data/restraints/parameters	7434/0/485
Goodness-of-fit on F ²	1.033
Final R indexes [I > 2σ (I)]	R ₁ = 0.0643, wR ₂ = 0.1902
Final R indexes [all data]	R ₁ = 0.0710, wR ₂ = 0.1986
Largest diff. peak/hole / e Å ⁻³	0.64/-0.30

X-ray crystallographic data for 4

Single crystal X-ray diffraction analysis. X-ray data for single crystals of **4** was recorded with a cryoloop mounted on a goniometer head in a cold stream of liquid nitrogen. The diffraction data were measured with synchrotron radiation with a Rayonix MX225HS CCD area detector with a silicon (111) double-crystal monochromator at the Pohang Accelerator Laboratory, Korea. The ADSC Quantum-210 ADX program was used for data collection and HKL3000sm was used for cell refinement, reduction, and absorption correction. The structure was solved by direct methods and refined by full-matrix least-squares analysis using anisotropic thermal parameters for non-hydrogen atoms with the SHELXTL

program. All hydrogen atoms were calculated at idealized positions and refined with the riding models. Also, C14, C34, O3A, and oxygen atom of water solvent(O8) is isotopically refined due to disorder. To account for this electron density, the program SQUEEZE, a part of the PLATON package of crystallographic software, was used to calculate the solvent disorder area and remove its contribution to the overall intensity data.^{S2}

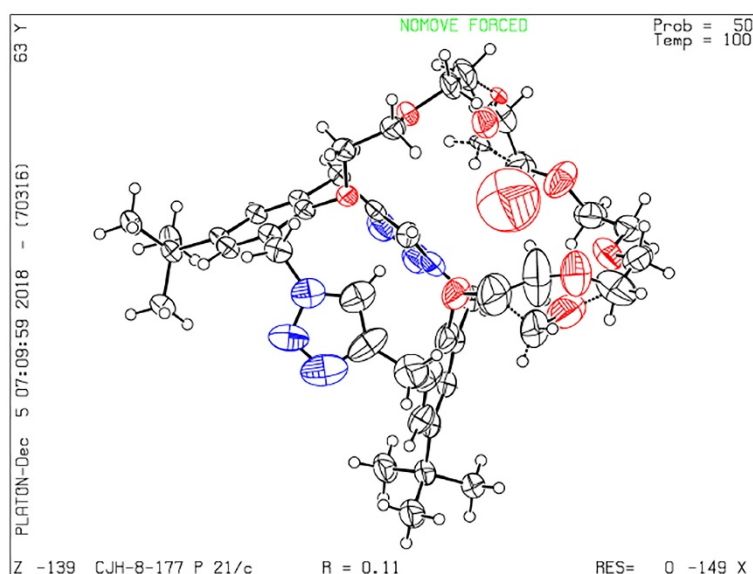


Figure S3. X-ray crystal structure of **4**. CCDC 1916784 (**4**) contains the supplementary crystallographic data for this paper. These data can be obtained free of charge from the Cambridge Crystallographic Data Centre via www.ccdc.cam.ac.uk/data_request/cif.

Table S3. Crystal data and structure refinement for **4**.

Empirical formula	C ₄₀ H ₅₄ N ₆ O ₈	
Formula weight	746.89	
Temperature	100(2) K	
Wavelength	0.700 Å	
Crystal system	Monoclinic	
Space group	P2 ₁ /c	
Unit cell dimensions	a = 9.6990(19) Å	α = 90°.
	b = 19.243(4) Å	β = 94.14(3)°.
	c = 21.345(4) Å	γ = 90°.

Volume	3973.4(14) Å ³
Z	4
Density (calculated)	1.249 Mg/m ³
Absorption coefficient	0.084 mm ⁻¹
F(000)	1600
Crystal size	0.111 x 0.109 x 0.054 mm ³
Theta range for data collection	1.884 to 28.790°.
Index ranges	-11<=h<=11, -23<=k<=23, -25<=l<=25
Reflections collected	29581
Independent reflections	8369 [R(int) = 0.0681]
Completeness to theta = 24.835°	96.9 %
Absorption correction	Empirical
Max. and min. transmission	1.000 and 0.965
Refinement method	Full-matrix least-squares on F ²
Data / restraints / parameters	8369 / 1 / 522
Goodness-of-fit on F ²	1.424
Final R indices [I>2sigma(I)]	R1 = 0.1082, wR2 = 0.3457
R indices (all data)	R1 = 0.1445, wR2 = 0.3798
Extinction coefficient	0.003(2)
Largest diff. peak and hole	0.997 and -0.784 e.Å ⁻³

X-ray crystallographic data for 7

Single crystal X-ray diffraction analysis. X-ray data for single crystals of **7** was recorded with a cryoloop mounted on a goniometer head in a cold stream of liquid nitrogen. The diffraction data were measured with synchrotron radiation with a Rayonix MX225HS CCD area detector with a silicon (111) double-crystal monochromator at the Pohang Accelerator Laboratory, Korea. The ADSC Quantum-210 ADX program was used for data collection and HKL3000sm was used for cell refinement, reduction, and absorption correction. The structure was solved by direct methods and refined by full-matrix least-squares analysis using anisotropic thermal parameters for non-hydrogen atoms with the SHELXTL program. Also, O4, C33, C34, C35, C36, C37, C38, C39, C40, and C41 are isotopically refined due to disorder. All hydrogen atoms except hydrogen atoms nearby disordered carbon atoms were calculated at idealized positions and refined with the riding models.

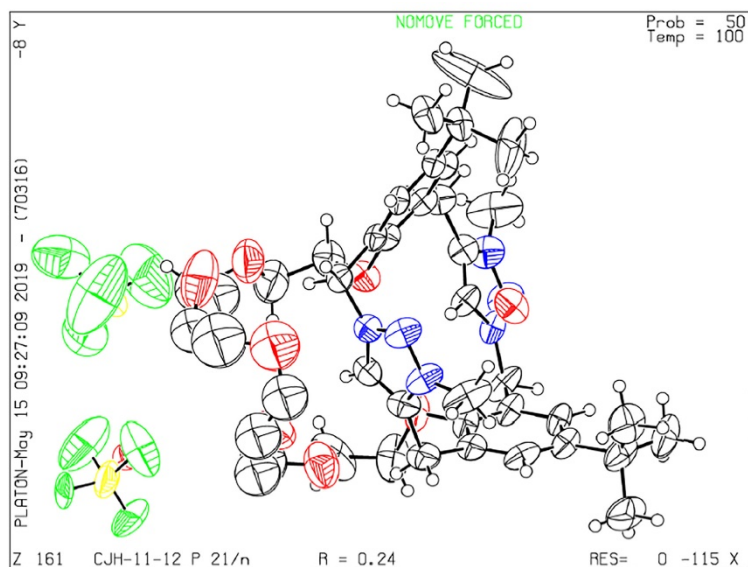


Figure S4. X-ray crystal structure of **7**. CCDC 1916785 (**7**) contains the supplementary crystallographic data for this paper. These data can be obtained free of charge from the Cambridge Crystallographic Data Centre via www.ccdc.cam.ac.uk/data_request/cif.

Table S4. Crystal data and structure refinement for **7**.

Empirical formula	C ₄₂ H ₄₈ B _{1.50} F ₆ N ₆ O ₉	
Formula weight	911.08	
Temperature	100(2) K	
Wavelength	0.700 Å	
Crystal system	Monoclinic	
Space group	P2 ₁ /n	
Unit cell dimensions	a = 12.961(3) Å	α = 90°.
	b = 19.320(4) Å	β = 93.98(3)°.
	c = 20.237(4) Å	γ = 90°.
Volume	5055.2(18) Å ³	
Z	4	
Density (calculated)	1.197 Mg/m ³	
Absorption coefficient	0.094 mm ⁻¹	
F(000)	1902	
Crystal size	0.442 x 0.314 x 0.283 mm ³	
Theta range for data collection	1.437 to 33.688°.	
Index ranges	-19 ≤ h ≤ 19, -27 ≤ k ≤ 27, -28 ≤ l ≤ 28	

Reflections collected	60064
Independent reflections	16244 [R(int) = 0.0387]
Completeness to theta = 24.835°	96.1 %
Absorption correction	Empirical
Max. and min. transmission	1.000 and 0.875
Refinement method	Full-matrix least-squares on F ²
Data / restraints / parameters	16244 / 0 / 579
Goodness-of-fit on F ²	2.254
Final R indices [$\gt 2\sigma(I)$]	R1 = 0.2412, wR2 = 0.5760
R indices (all data)	R1 = 0.2805, wR2 = 0.6016
Extinction coefficient	0.104(15)
Largest diff. peak and hole	2.404 and -0.891 e.Å ⁻³

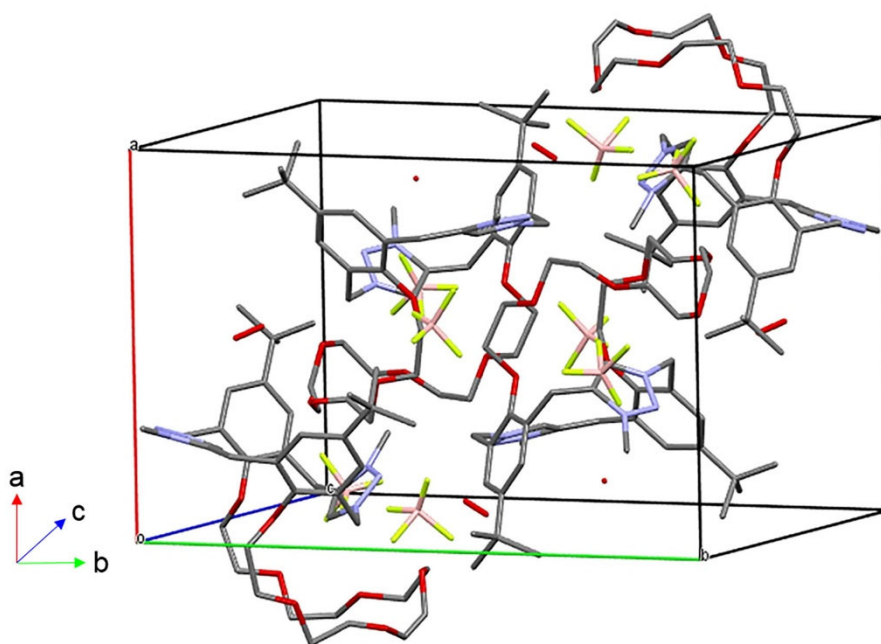


Figure S5. Crystal packing diagram of the unit cell of **7**. The hydrogen atoms are omitted for clarity.

3. NOESY spectral analysis

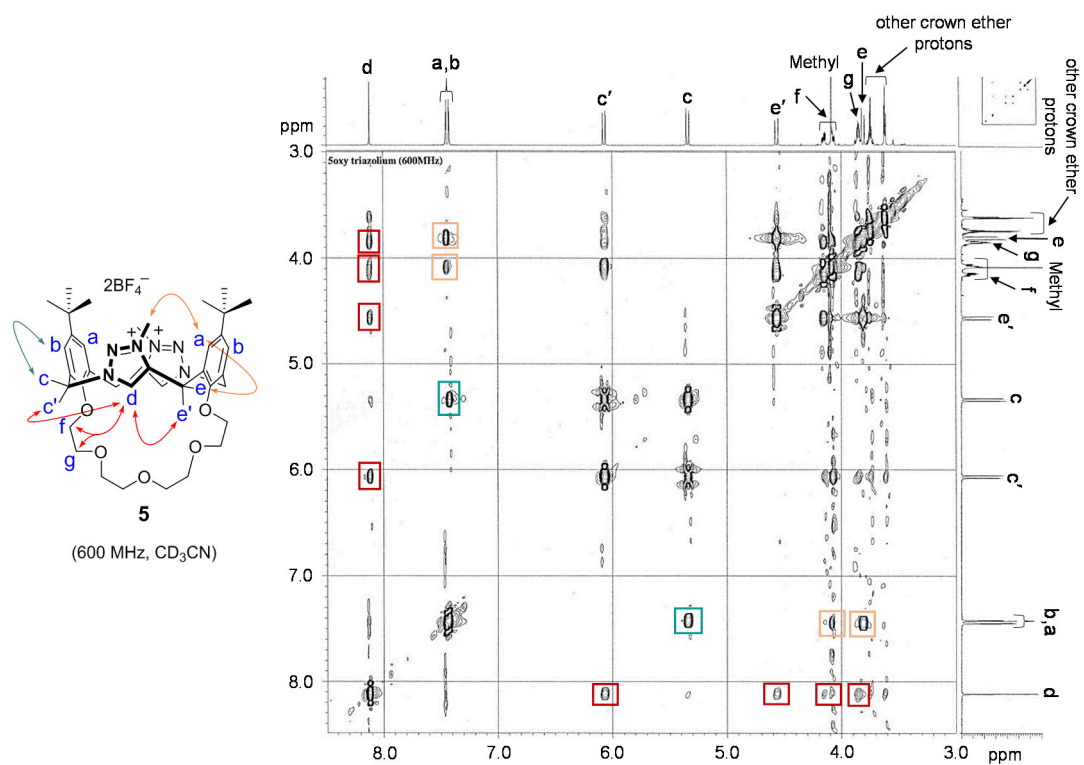


Figure S6. ^1H - ^1H NOESY NMR spectra of **5**.

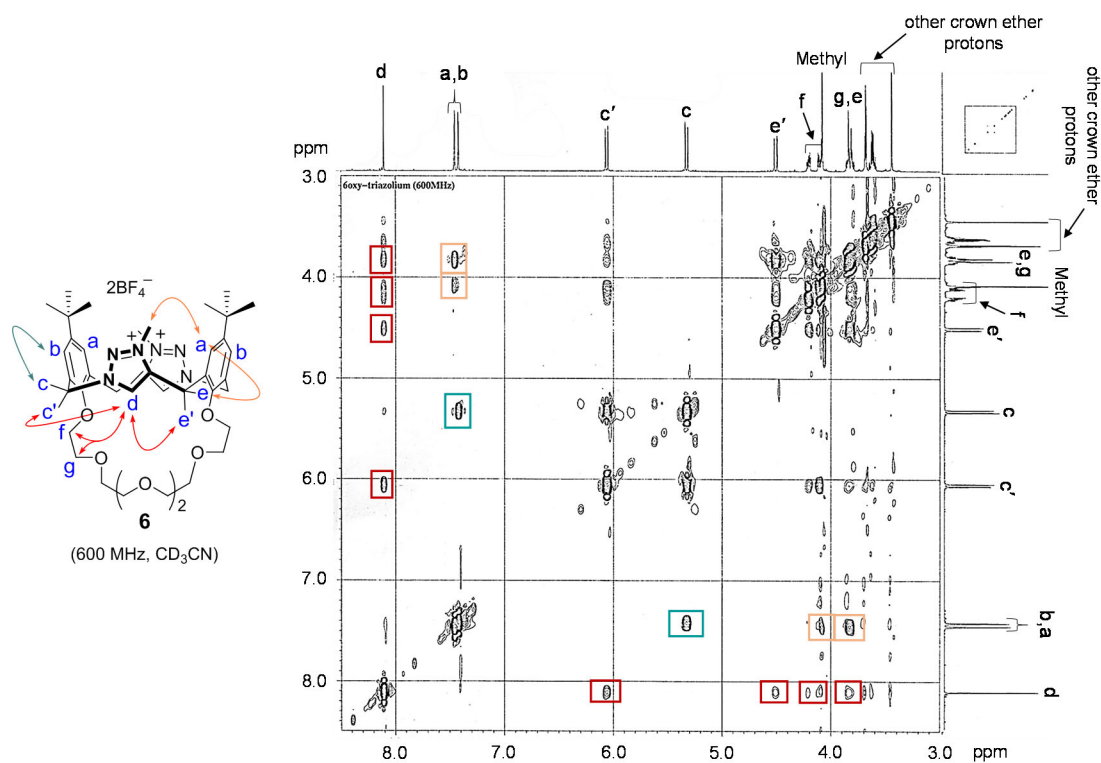


Figure S7. ^1H - ^1H NOESY NMR spectra of **6**.

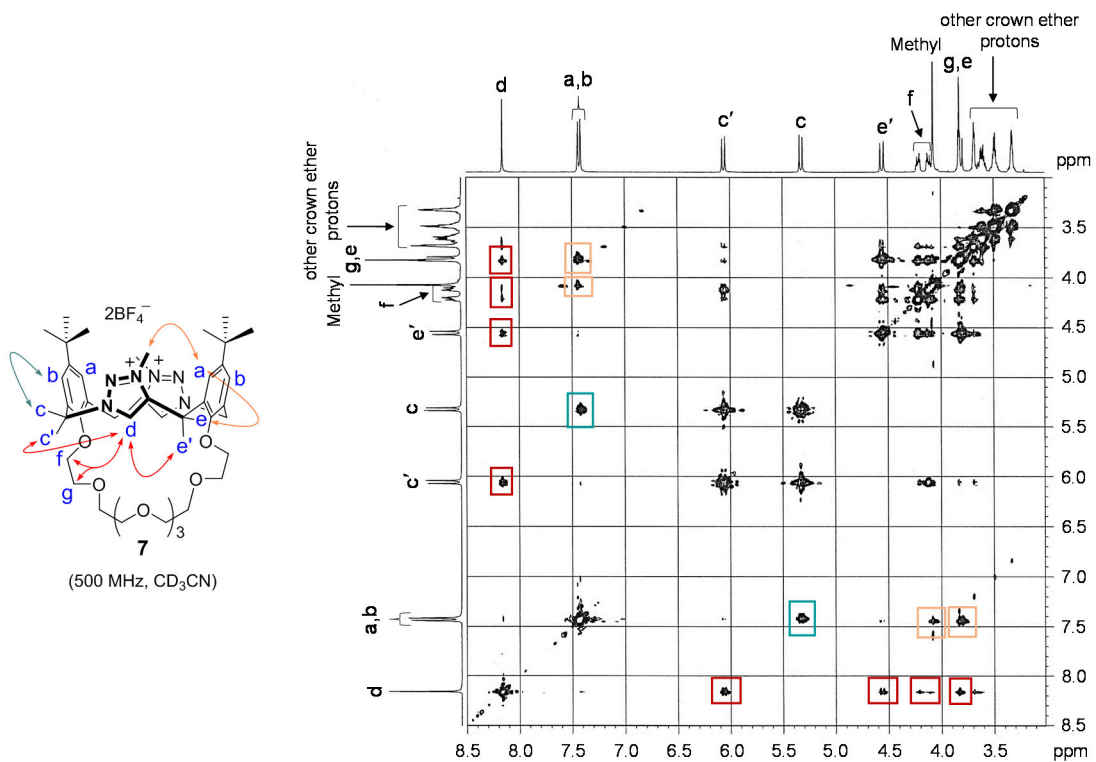


Figure S8. ^1H - ^1H NOESY NMR spectra of **7**.

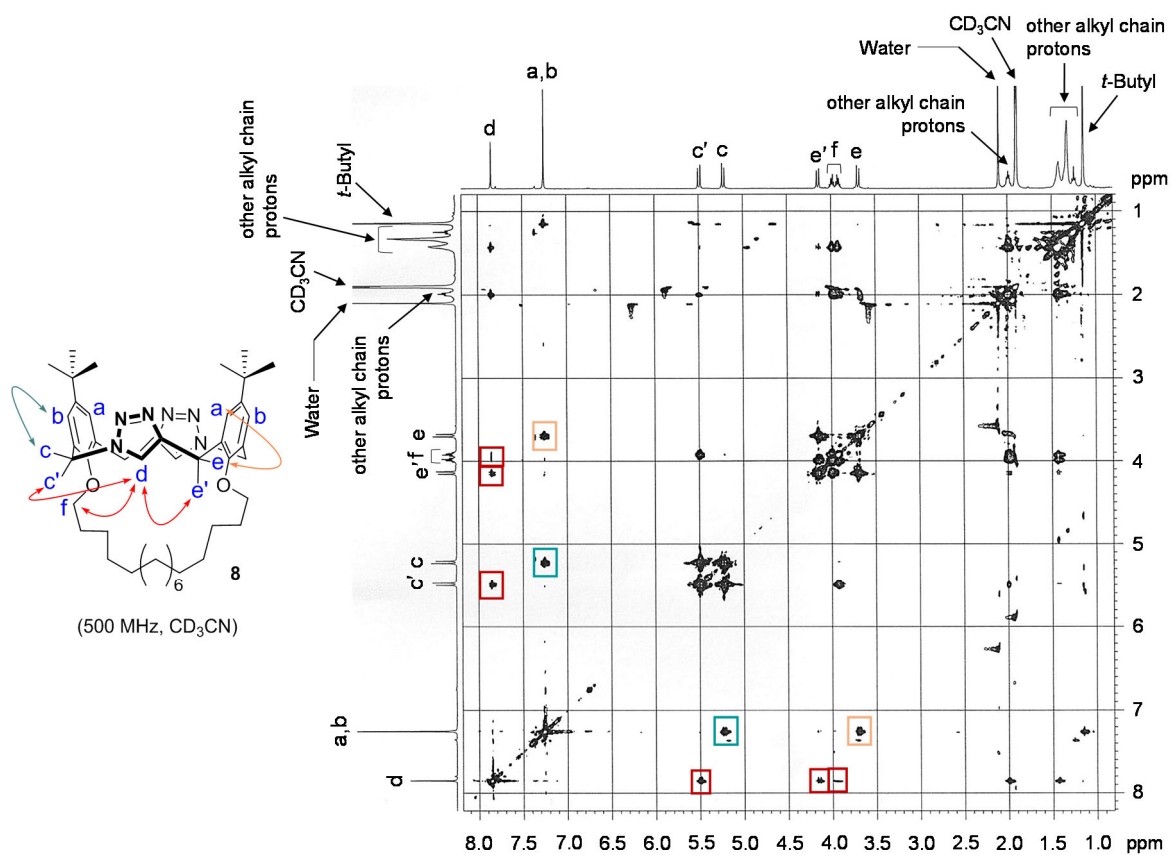


Figure S9. ^1H - ^1H NOESY NMR spectra of **8**.

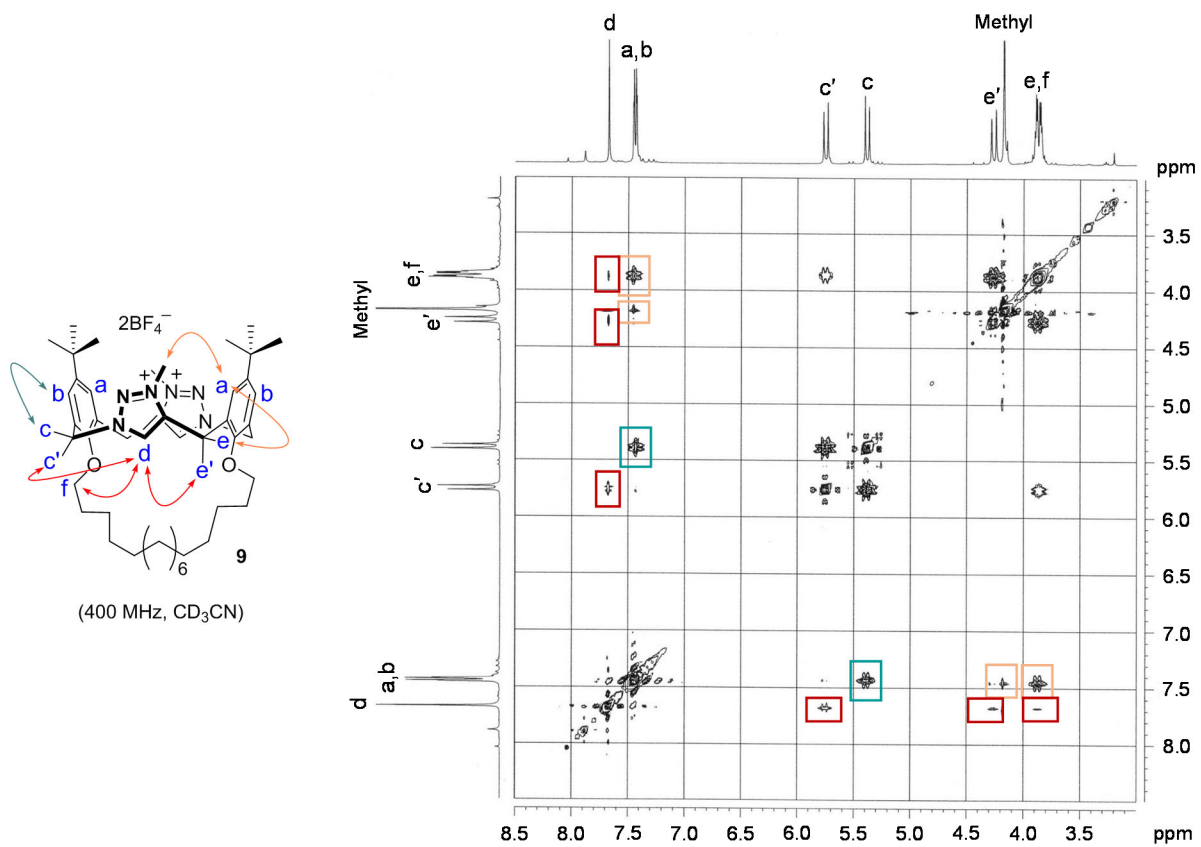


Figure S10. ^1H - ^1H NOESY NMR spectra of **9**.

4. Details of NMR spectroscopic binding studies

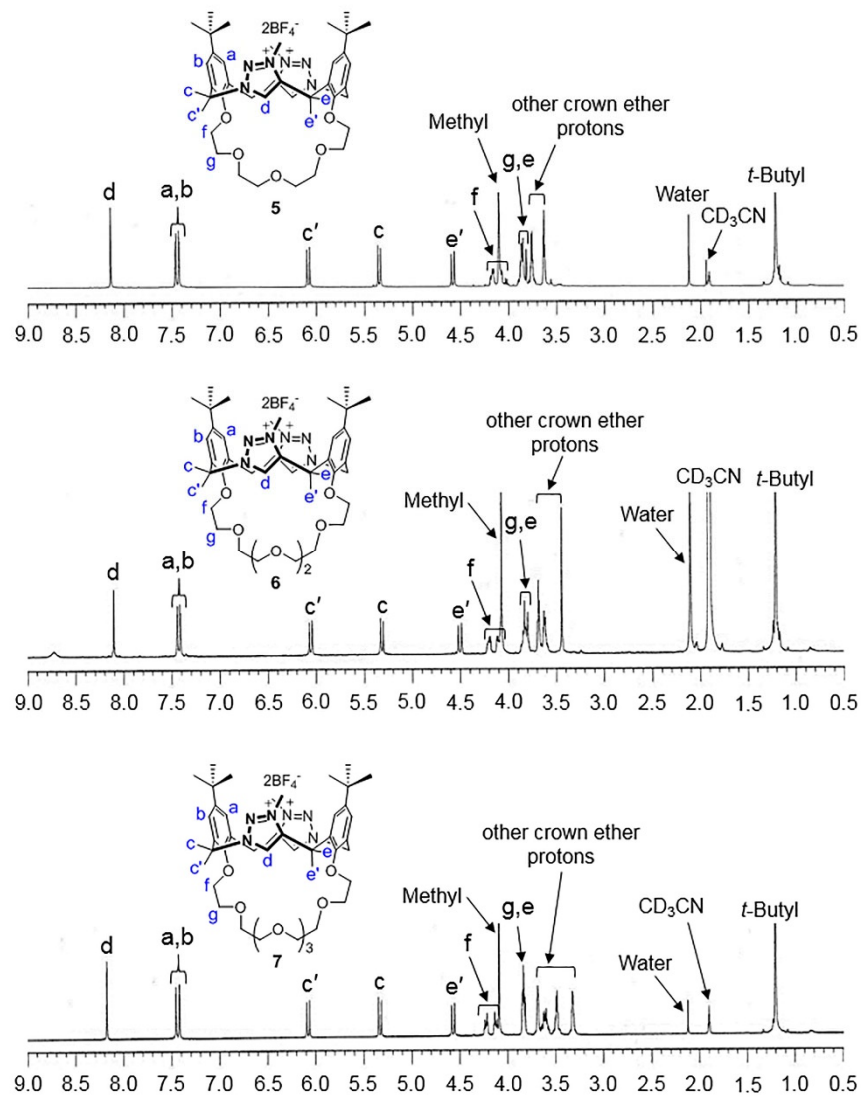


Figure S11. ^1H NMR spectra of **5**, **6** and **7** in CD_3CN (1 mM).

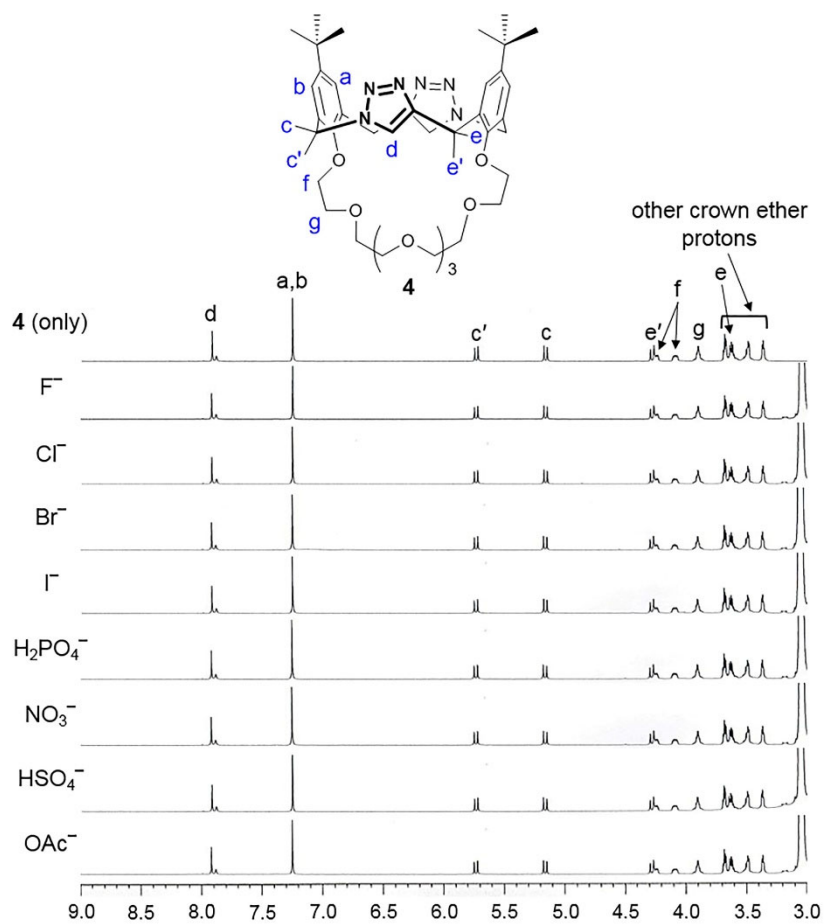


Figure S12. ^1H NMR spectra of **4** in CD_3CN (1 mM) in the presence of various anions (F^- , Cl^- , Br^- , I^- , H_2PO_4^- , NO_3^- , HSO_4^- and OAc^- (10 equiv)).

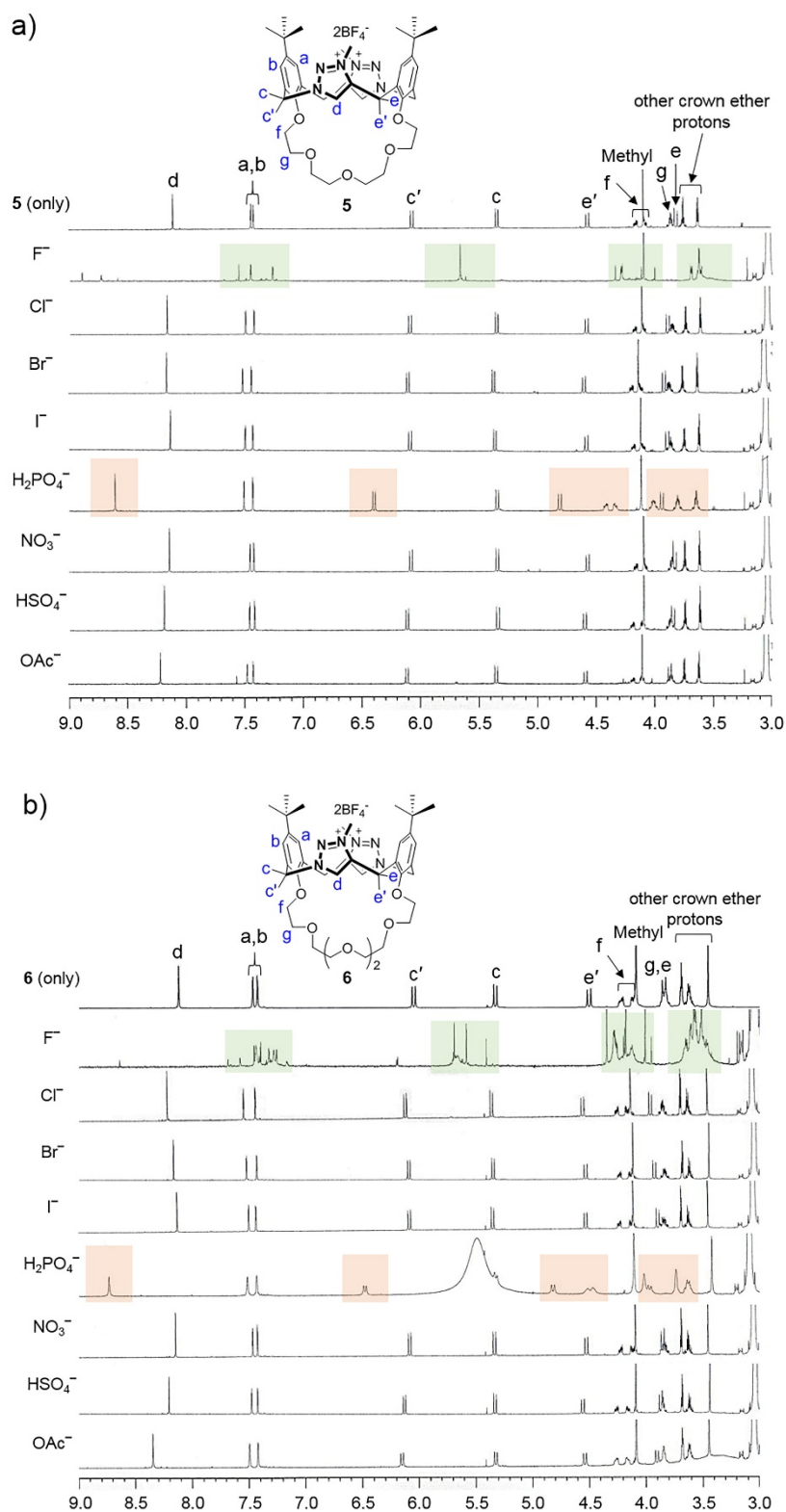
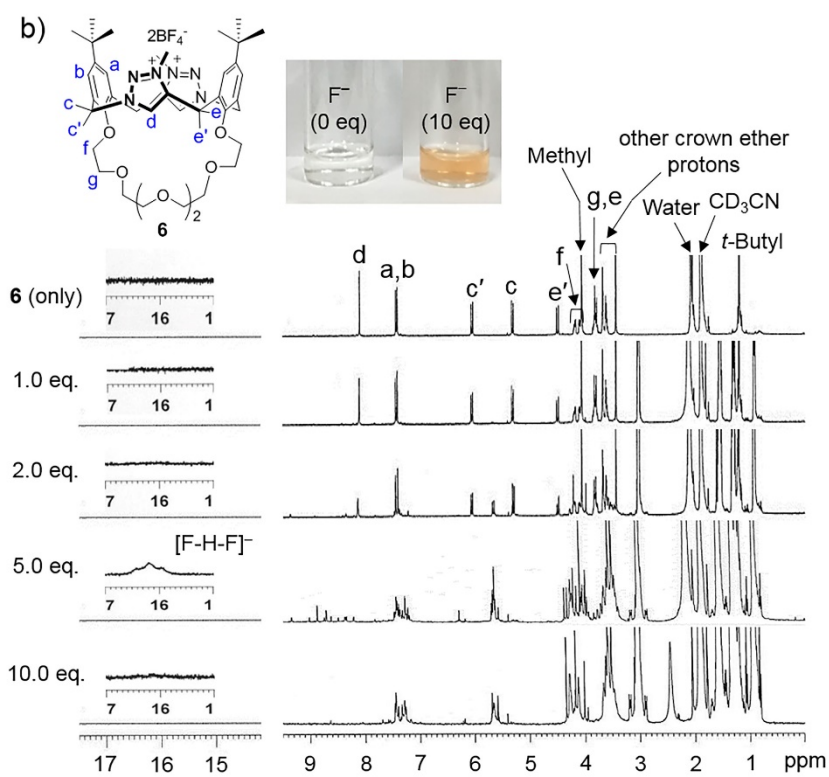
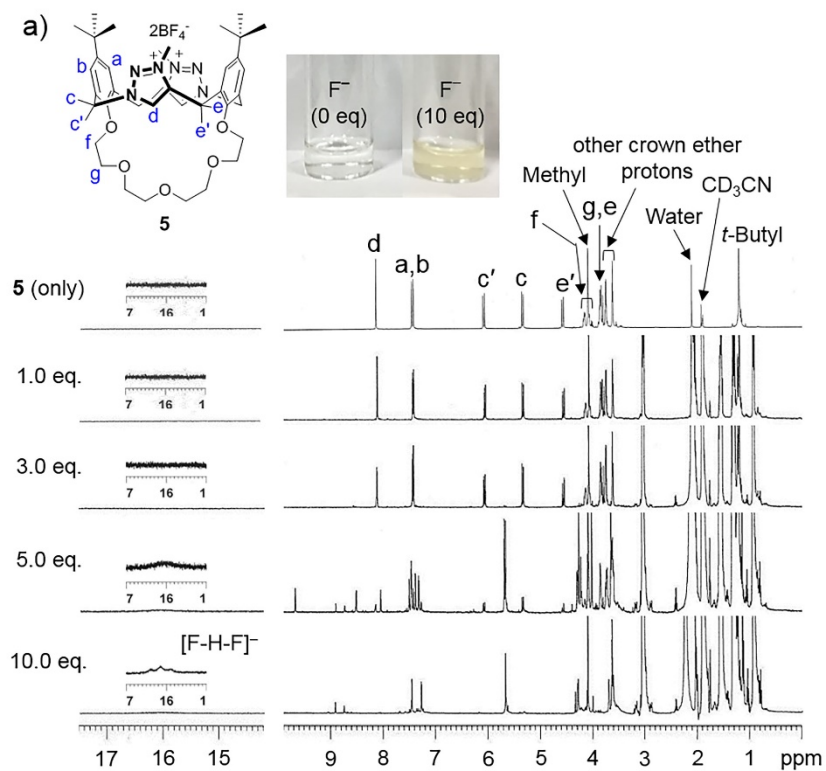


Figure S13. 1H NMR spectra of (a) **5** and (b) **6** in CD_3CN (1 mM) in the presence of various anions (F^- , Cl^- , Br^- , I^- , $H_2PO_4^-$, NO_3^- , HSO_4^- and OAc^- (10 equiv)).



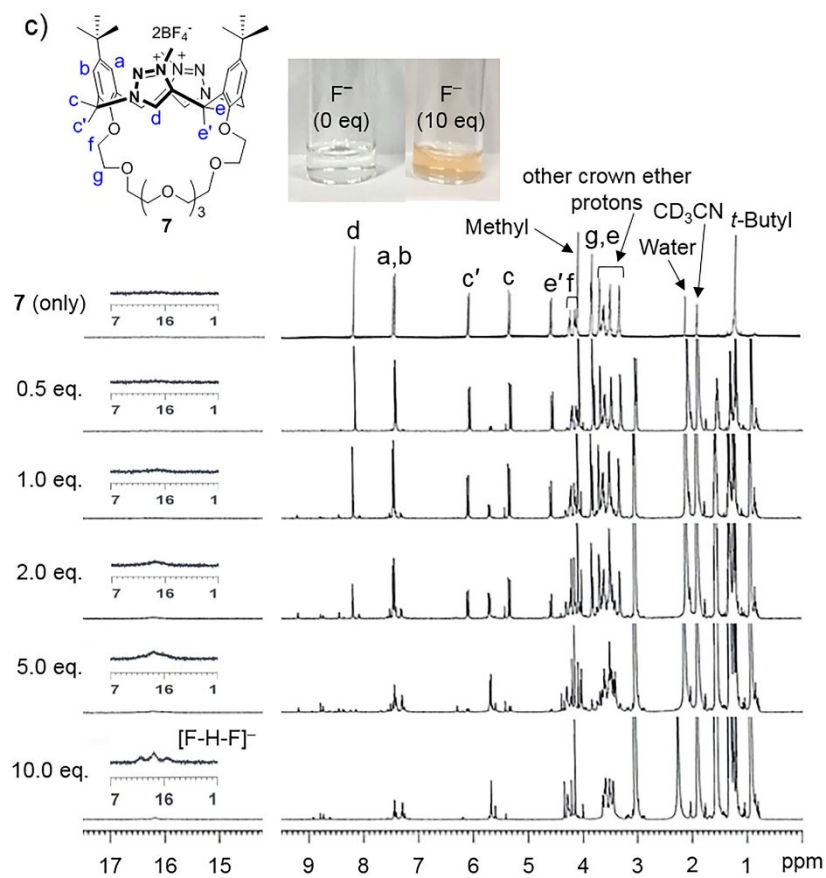


Figure S14. ^1H NMR spectra of (a) **5**, (b) **6** and (c) **7** in CD_3CN (1 mM) recorded in the presence of increasing concentrations of F^- anion.

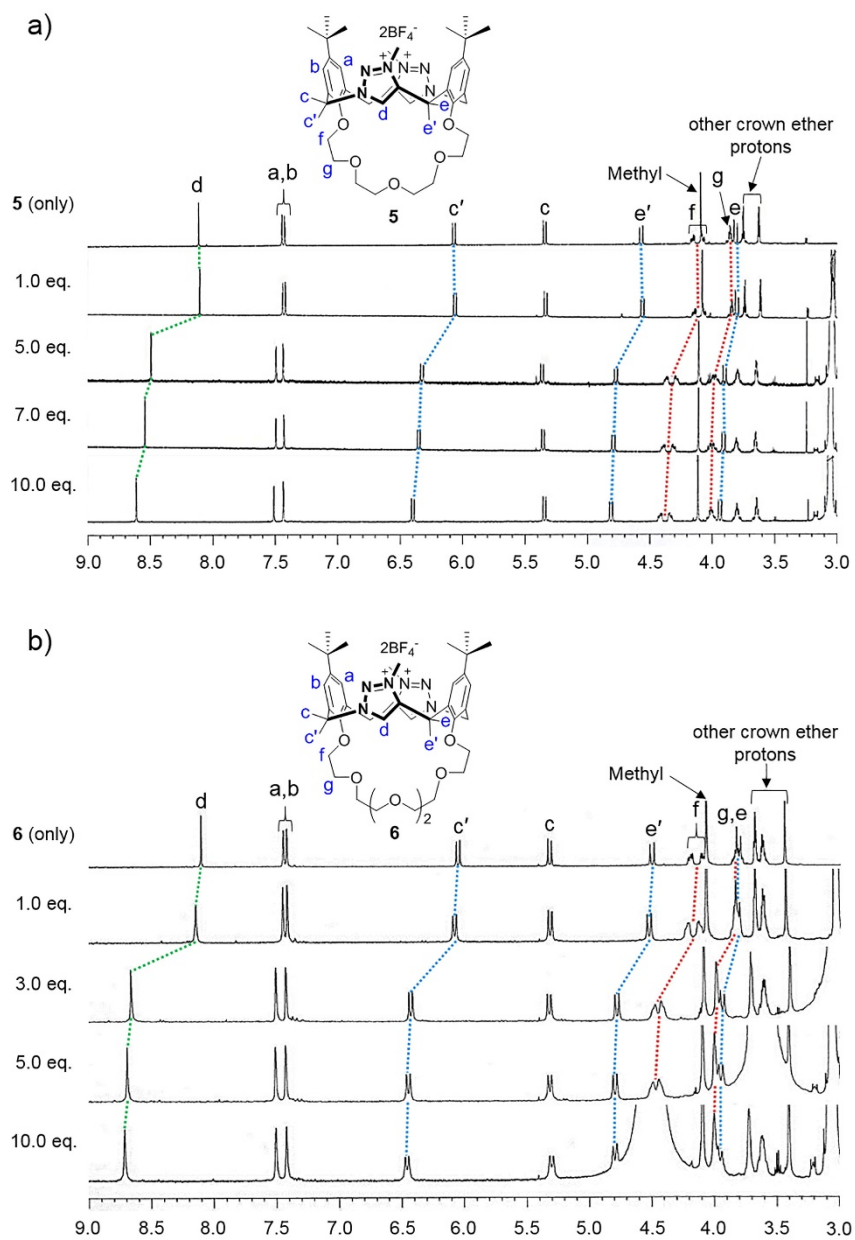


Figure S15. ^1H NMR spectra of (a) **5** and (b) **6** in CD_3CN (1 mM) recorded in the presence of increasing concentrations of H_2PO_4^- anion.

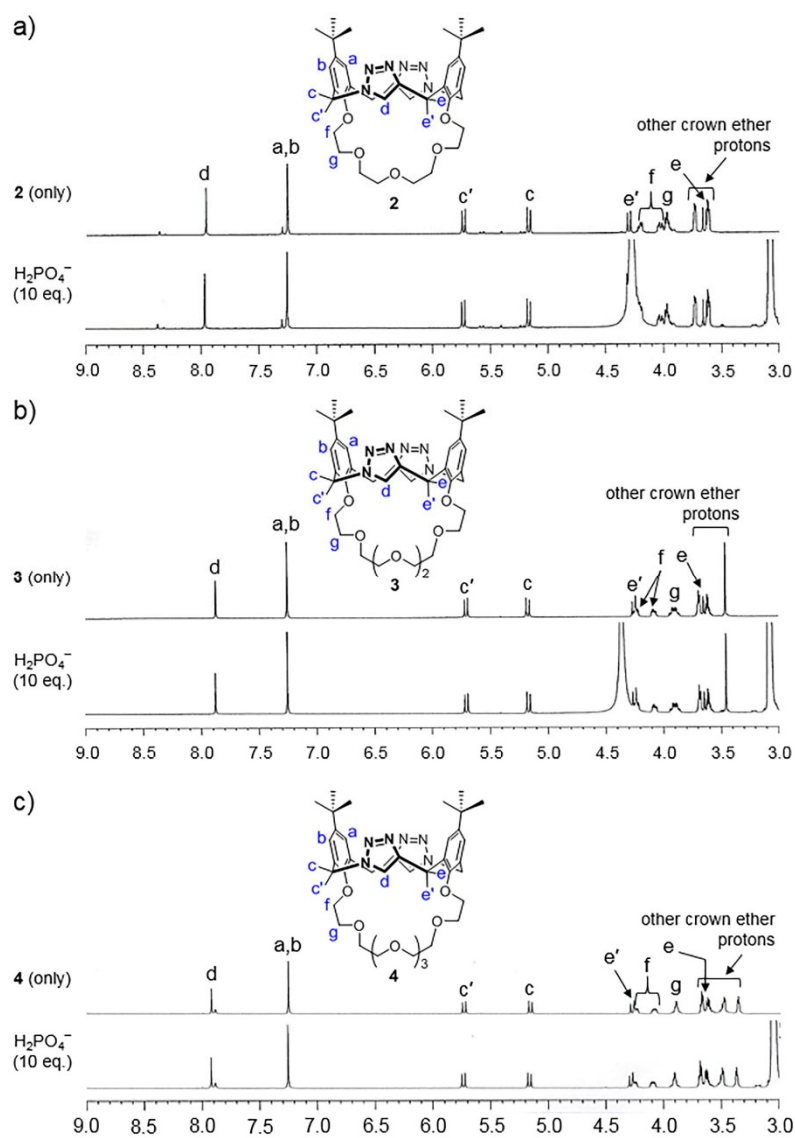


Figure S16. ^1H NMR spectrum of (a) **2**, (b) **3** and (c) **4** in CD_3CN (1 mM) in the presence of H_2PO_4^- anion (10 equiv).

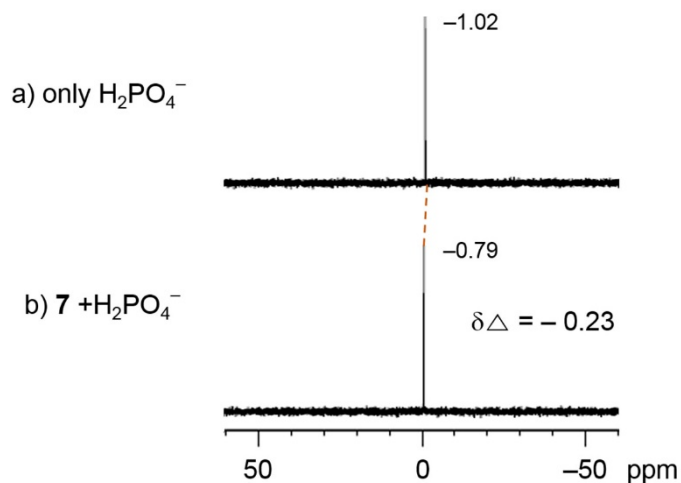


Figure S17. ^{31}P NMR spectra of (a) H_2PO_4^- (2 mM) and (b) with 0.5 equiv. of receptor **7** (1 mM) in CD_3CN .

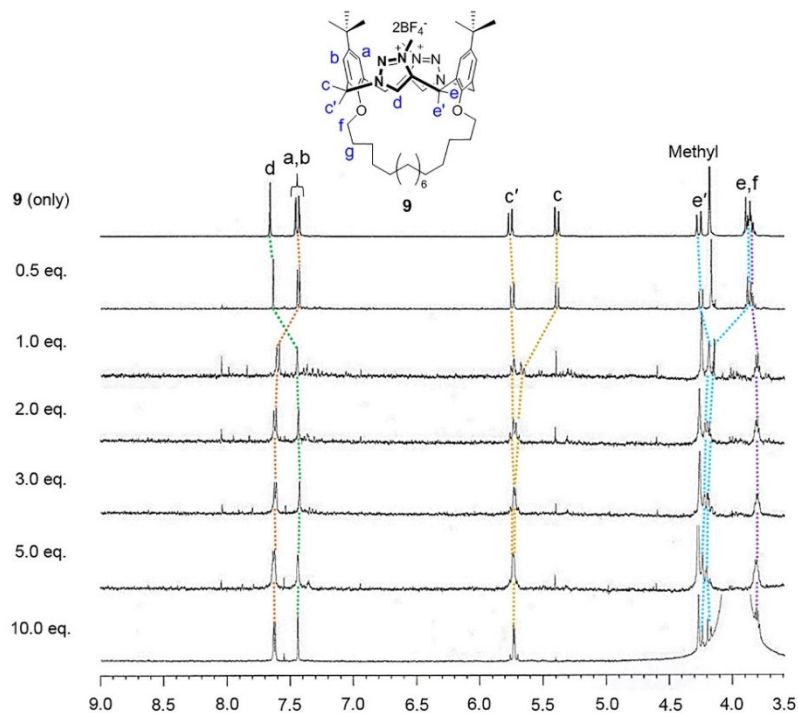


Figure S18. ^1H NMR spectra of **9** in CD_3CN (1 mM) recorded in the presence of increasing concentrations of H_2PO_4^- anion.

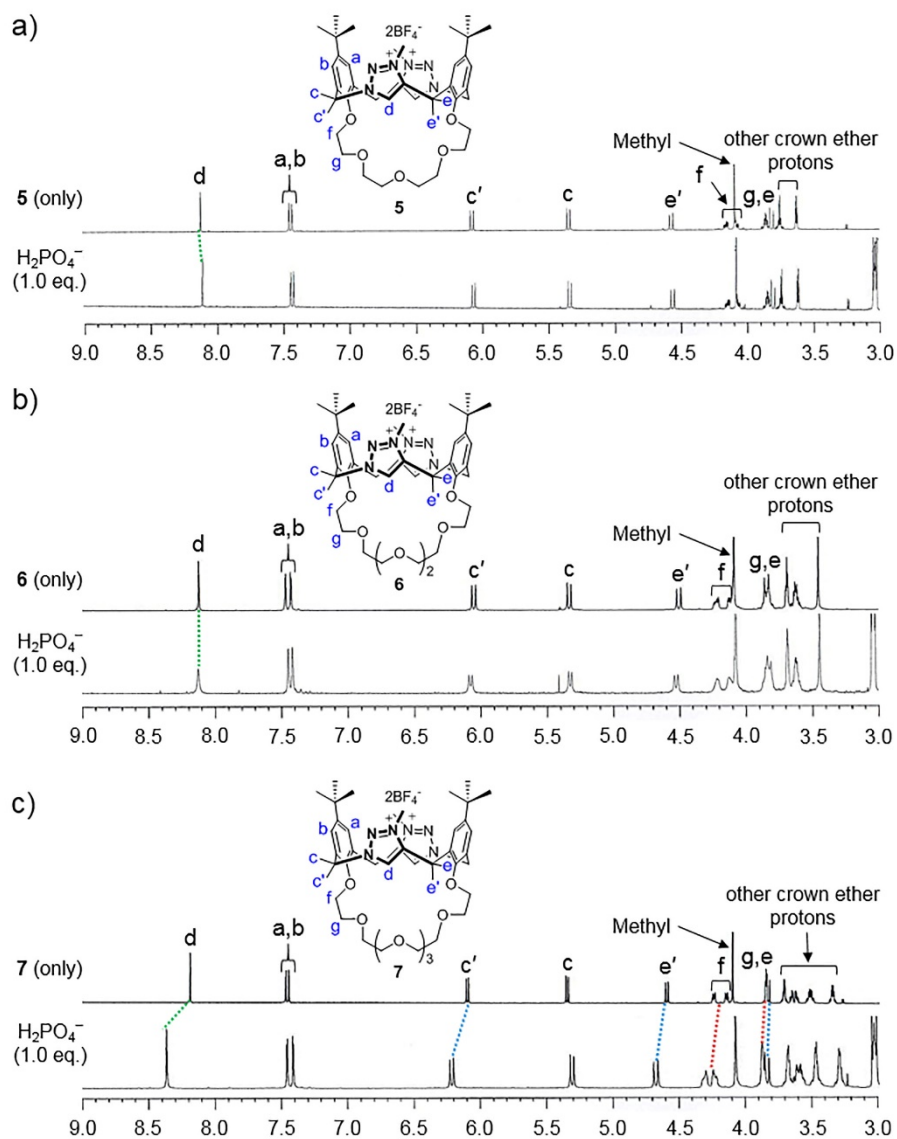


Figure S19. ^1H NMR spectrum of (a) **5**, (b) **6** and (c) **7** in CD_3CN (1 mM) in the presence of H_2PO_4^- anion (1 equiv).

5. Titration experiment

(1) ^1H NMR studies

Job's plot for the binding stoichiometric ratio: Stock solutions of equal concentration of triazolium crown ether **7** (1 mM) and TBA- H_2PO_4 (1 mM) in CD_3CN were prepared separately. Ten NMR tubes were each filled with a total 550 μL solution of triazolium crown ether **7** and TBA- H_2PO_4 in the following ratios (**7** : TBA- H_2PO_4): 10:0, 9:1, 8:2, 7:3, 6:4, 5:5, 4:6, 3:7, 2:8, 1:9. Job's plot was constructed by plotting chemical shift of triazolium C₅-H signal against the molar fraction of the host.

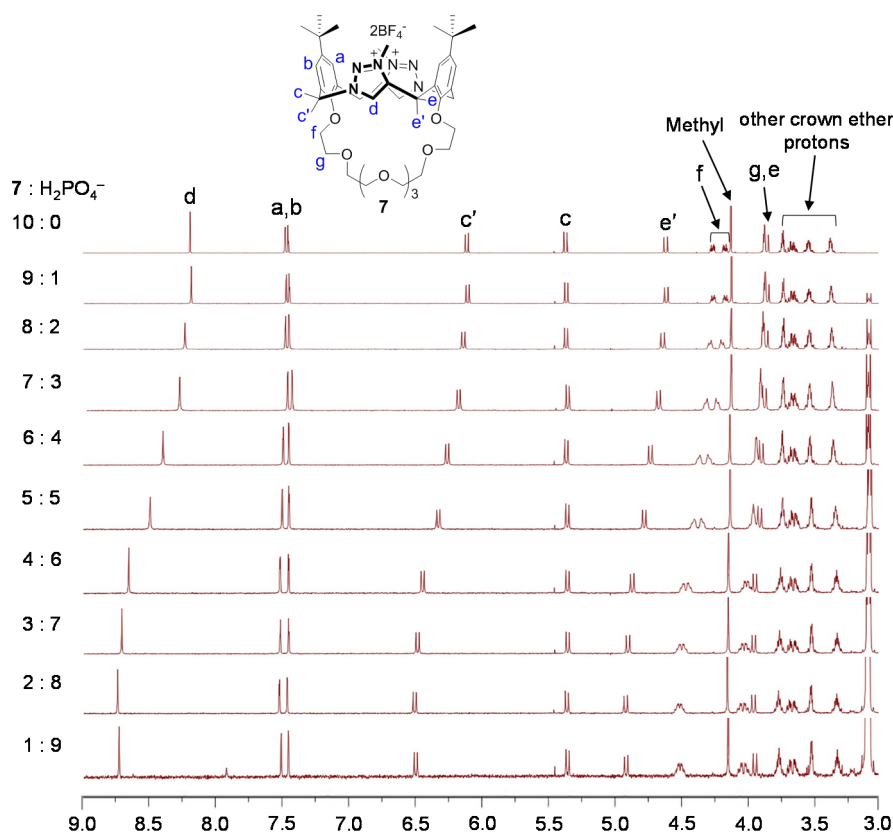


Figure S20. ^1H NMR titration data of **7** with TBA- H_2PO_4 in CD_3CN for the construction of the Job's plot.

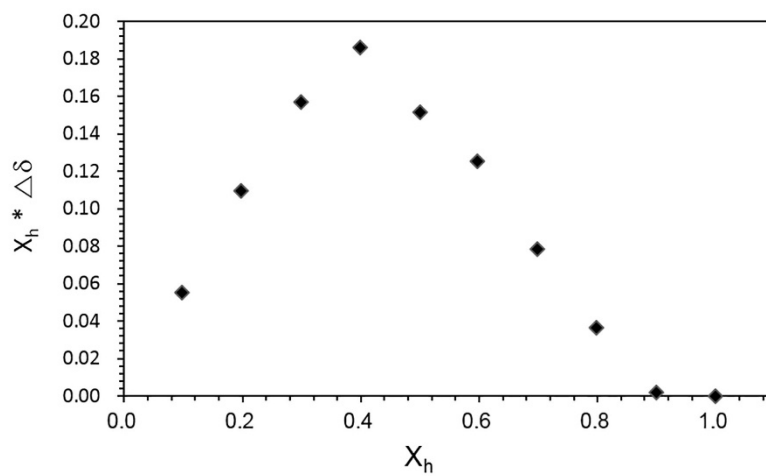


Figure S21. Job's plot generated from the ^1H NMR titration data of **7** with TBA- H_2PO_4 in CD_3CN .

^1H NMR titration of 7 with TBA- H_2PO_4 : Triazolium crown ether **7** and TBA- H_2PO_4 were dissolved in CD_3CN to prepare stock solutions of **7** (1 mM) and TBA- H_2PO_4 (10 mM). The requisite number of NMR samples were prepared adding increasing amounts of the TBA- H_2PO_4 stock solution (0-270 μL) to 530 μL of stock solution of **7**. The binding constant was analyzed by Bindfit, plotting chemical shift of triazolium $\text{C}_5\text{-H}$ signal against equivalents of the anion added.

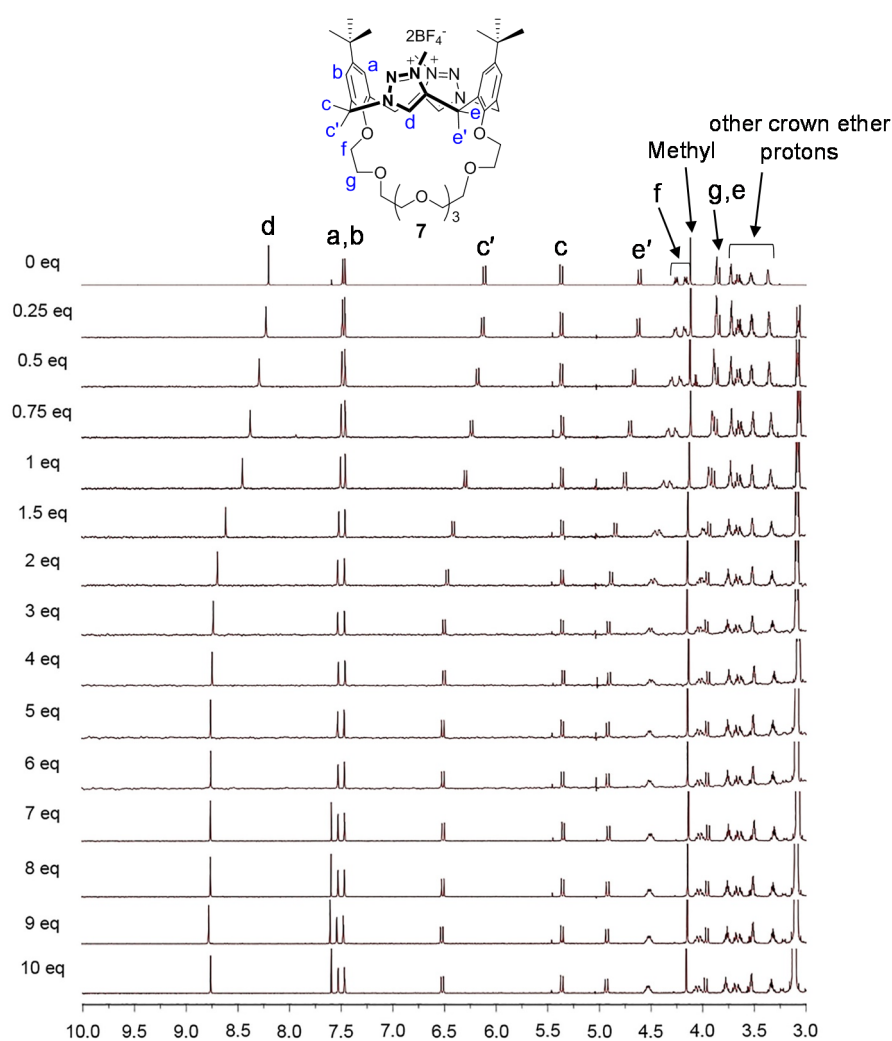


Figure S22. ^1H NMR titration experiment of **7** with TBA- H_2PO_4 in CD_3CN .



Figure S23. Screenshot of the summary window of <http://app.supramolecular.org/bindfit/>. This screenshot shows the raw data for ¹H NMR titration of **7** with H₂PO₄⁻ following the triazolium C5–H signal vs. the data fitted to 1 : 2 NMR binding model, the corresponding residual plot and the association constants with the calculated asymptotic standard errors.

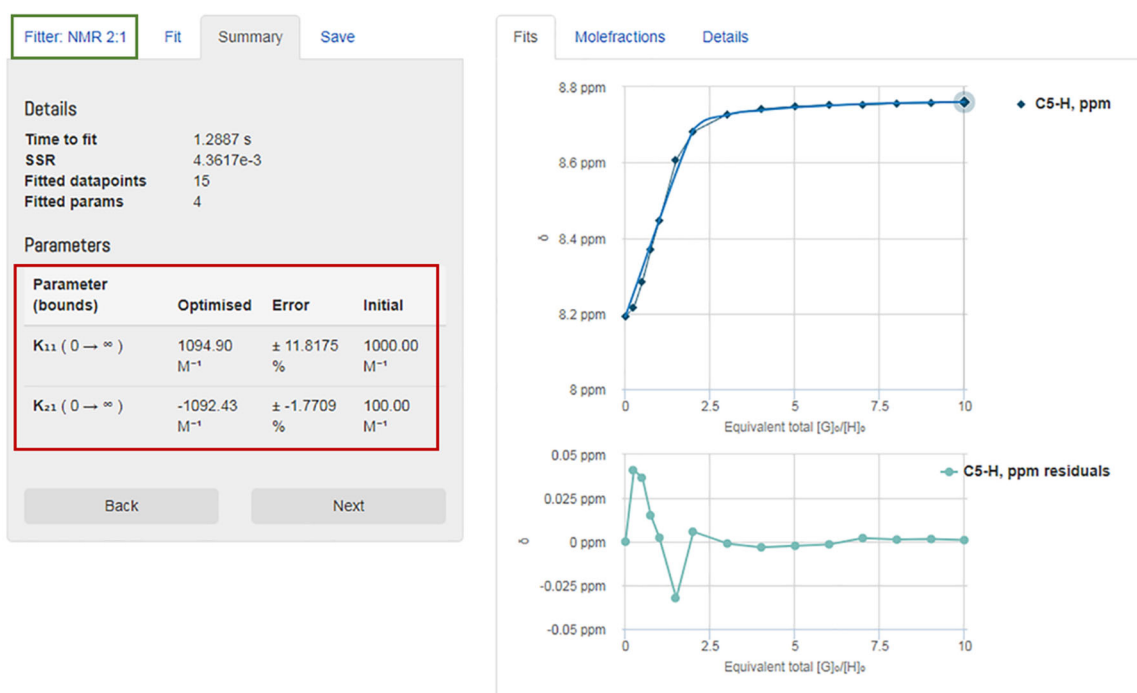


Figure S24. Screenshot of the summary window of <http://app.supramolecular.org/bindfit/>. This screenshot shows the raw data for ¹H NMR titration of **7** with H₂PO₄⁻ following the triazolium C5–H signal vs. the data fitted to 2 : 1 NMR binding model, the corresponding residual plot and the association constants with the calculated asymptotic standard errors.



Figure S25. Screenshot of the summary window of <http://app.supramolecular.org/bindfit/>. This screenshot shows the raw data for ^1H NMR titration of **7** with H_2PO_4^- following the triazolium C5–H signal vs. the data fitted to 1 : 1 NMR binding model, the corresponding residual plot and the association constants with the calculated asymptotic standard errors.

Table S5. Summary of association constants of **7** for H_2PO_4^- according to different binding models.^a

Receptor	Binding models		
	1 : 1	1 : 2	2 : 1
7	K_{11} 2971.88 ($\pm 29.86\%$)	K_{11} 217458.66 ($\pm 481.53\%$)	K_{11} 1094.90 ($\pm 11.82\%$)
		K_{12} 48731.08 ($\pm 98.65\%$)	K_{21} -1092.43 ($\pm -1.77\%$)

^a The Bindfit software for data analysis was used from *supramolecular.org*.

(2) UV-vis studies

Job's plot for the binding stoichiometric ratio: Stock solutions of equal concentration of triazolium crown ether **7** (10 μM) and TBA- H_2PO_4 (10 μM) in acetonitrile were prepared separately. Keeping the total volume of 3 mL, aliquots of two stock solutions were added to a cuvette in different ratios. A Job's plot was constructed by plotting UV absorbance at 220 nm against the molar fraction of the host.

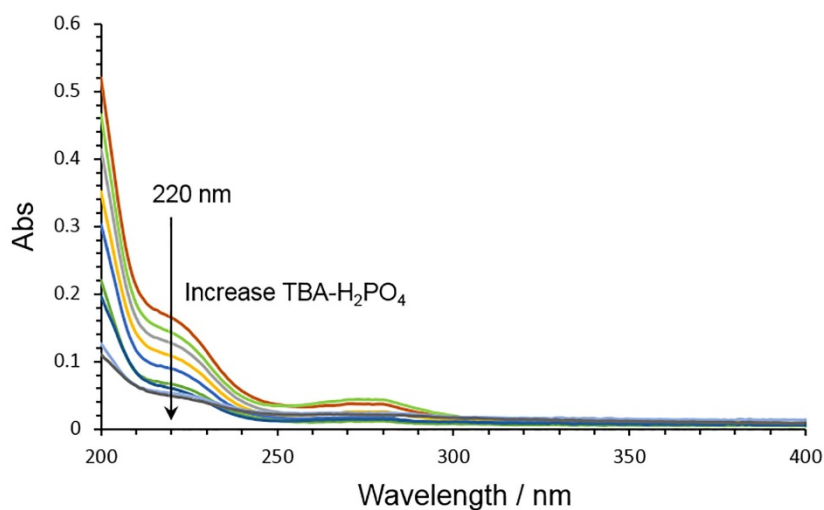


Figure S26. UV absorbance changes of **7** with TBA- H_2PO_4 in acetonitrile for the construction of the Job's plot.

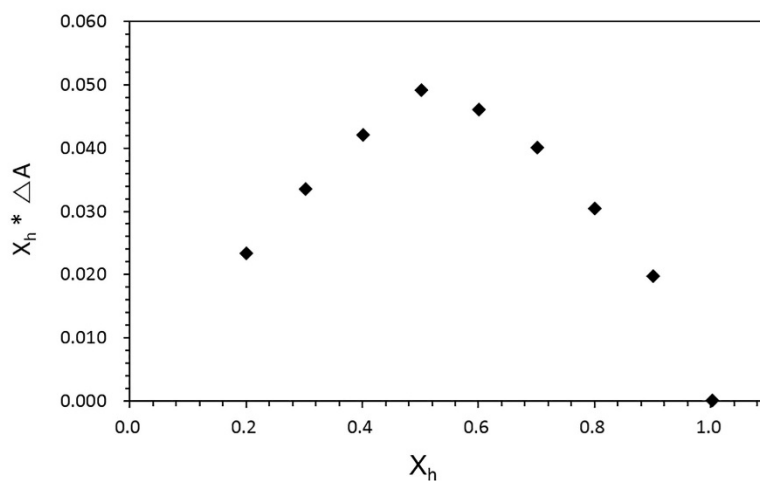


Figure S27. Job's plot generated from the UV-vis titration data of **7** with TBA- H_2PO_4 in acetonitrile.

UV-vis titration of 7 with TBA-H₂PO₄: Stock solutions of triazolium crown ether 7 (10 μ M) and TBA-H₂PO₄ (1 mM) in acetonitrile were prepared separately. A 3 mL of the host (triazolium crown ether 7) solution was transferred to a cuvette and an initial spectrum was taken. Aliquots of the guest (TBA-H₂PO₄) solution (15–600 μ L) were added to the cuvette and the spectrum was recorded after each addition. The binding constant was analyzed by Bindfit, plotting UV absorbance at 220 nm against equivalents of the anion added.

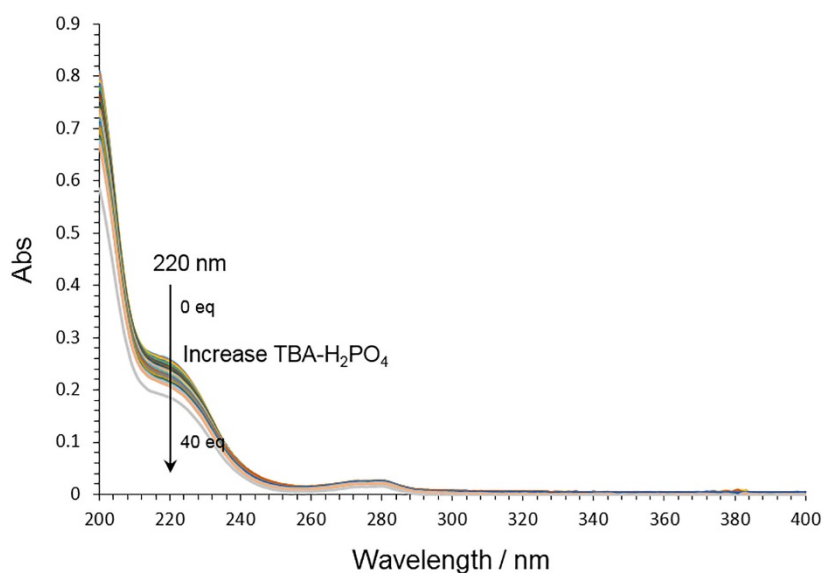


Figure S28. UV absorbance changes of 7 with increasing the amount of TBA-H₂PO₄ in acetonitrile.



Figure S29. Screenshot of the summary window of <http://app.supramolecular.org/bindfit/>. This screenshot shows the raw data for UV-vis titration of **7** with H_2PO_4^- following the UV absorbance signal at 220nm vs. the data fitted to 1 : 1 UV binding model, the corresponding residual plot and the association constants with the calculated asymptotic standard errors.

6. Detection limit measurements

The detection limit of H_2PO_4^- by **7** ($10 \mu\text{M}$) in acetonitrile was determined using the equation: $\text{LOD} = 3\sigma/K$, where σ denotes the standard deviation of blank solution (without analyte), K is the slope between UV absorbance intensity and H_2PO_4^- concentration. The σ was obtained from the results of 20 separate measurements.

Receptor	Slope, K	R^2	Standard deviation, σ	Limit of detection (LOD) (μM)
7	0.0002	0.9301	0.00029	4.35

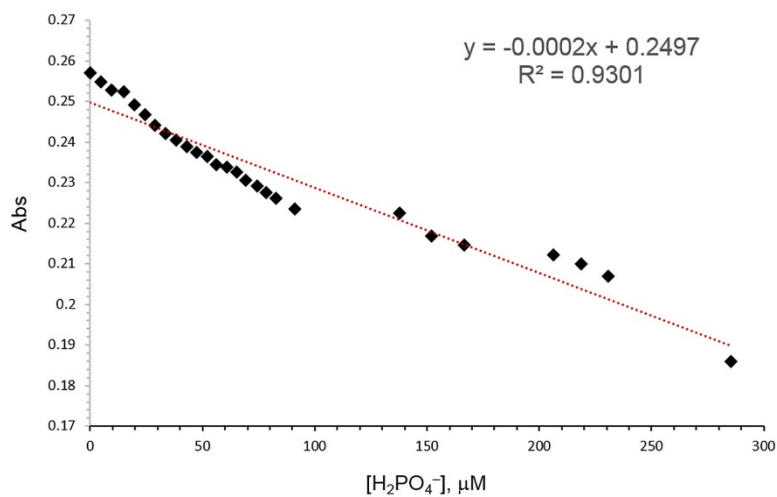


Figure S30. Calibration curve of **7** ($10 \mu\text{M}$) in acetonitrile. The UV absorbance intensities of **7** was recorded at 220 nm.

7. Theoretical studies

Calculation details. DFT calculations of **7** and $7\text{-H}_2\text{PO}_4^-$ were performed at the CAM-B3LYP/6-31+G(d,p) level of theory,^{S3} in acetonitrile (IEFPCM),^{S4} using the Gaussian 16 software suite,^{S5} starting from the crystal structure geometry of **4**. Input files were generated using Gabedit 2.5.0^{S6} and final geometries were visualized using GaussView 6.0^{S7} and Gabedit 2.5.0.

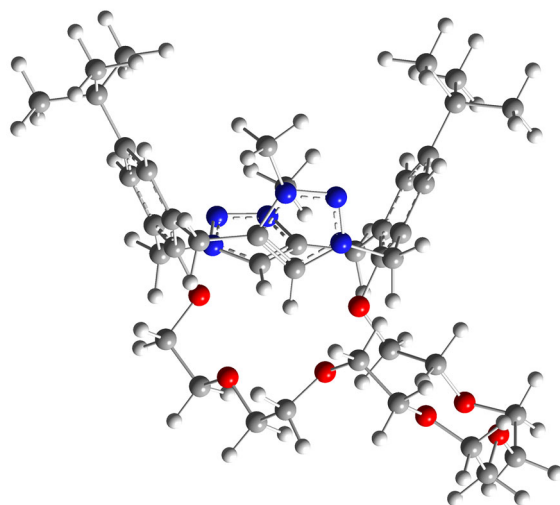


Figure S31. Ball and stick model of DFT-optimized structure of **7**.

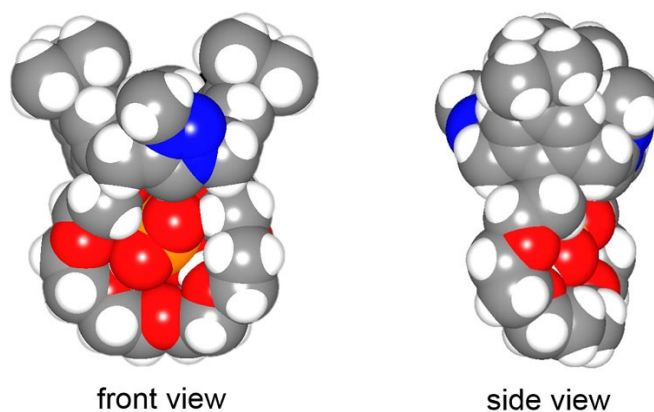


Figure S32. Space filling model of DFT-optimized structure of $7\text{-H}_2\text{PO}_4^-$ at the CAM-B3LYP/6-31+G(d,p) level of theory in acetonitrile.

8. Simulated ^1H NMR spectra

Calculation details. NMR calculation were performed at the PBE0/cc-PVTZ level of theory^{S8} in acetonitrile (IEFPCM), using the CSGT method^{S9} on the CAM-B3LYP/6-31+G(d,p)-optimized geometries using the Gaussian 16 software suite. Calculations omitted spin-spin interactions (NMR shielding only). The ppm values were obtained relative to tetramethylsilane, calculated in the same manner. The ppm values for chemically equivalent protons were averaged out and a theoretical NMR spectrum was constructed using a gaussian distribution with a standard deviation of 0.01 ppm, and an intensity proportional to the number of equivalent protons.

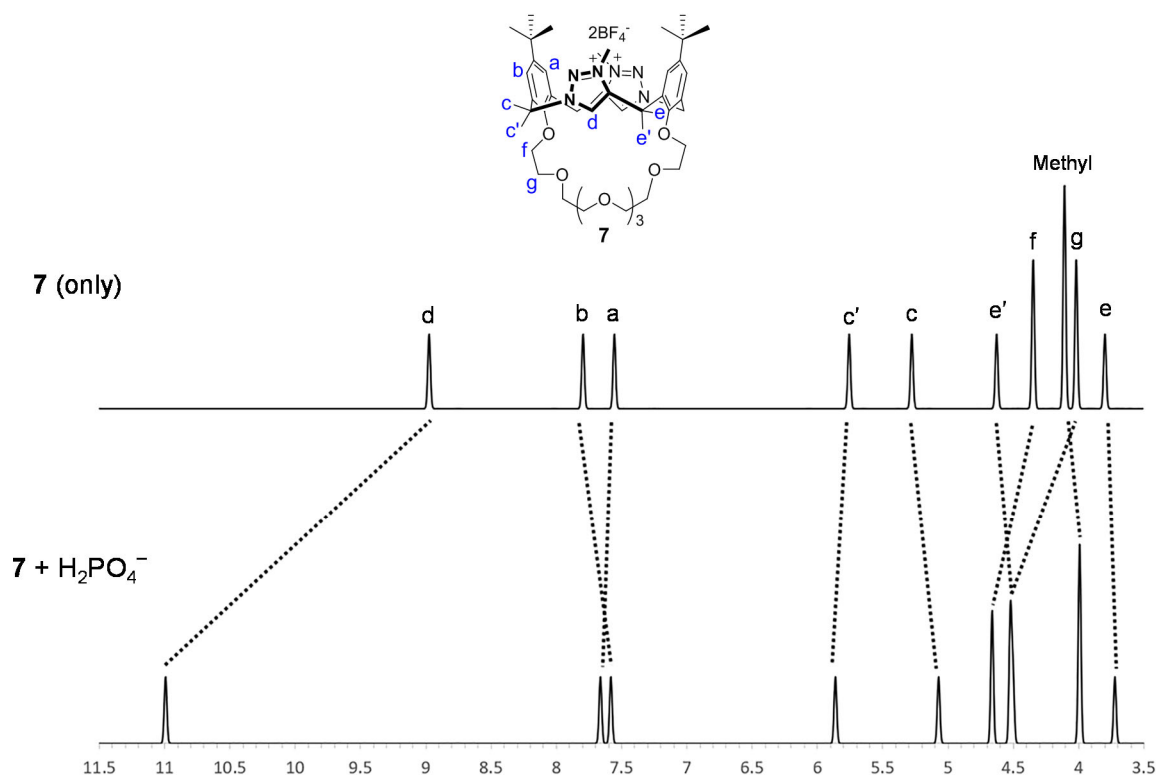


Figure S33. Simulated ^1H NMR spectra of **7** and the **7**- H_2PO_4^- complex.

9. NMR Spectra

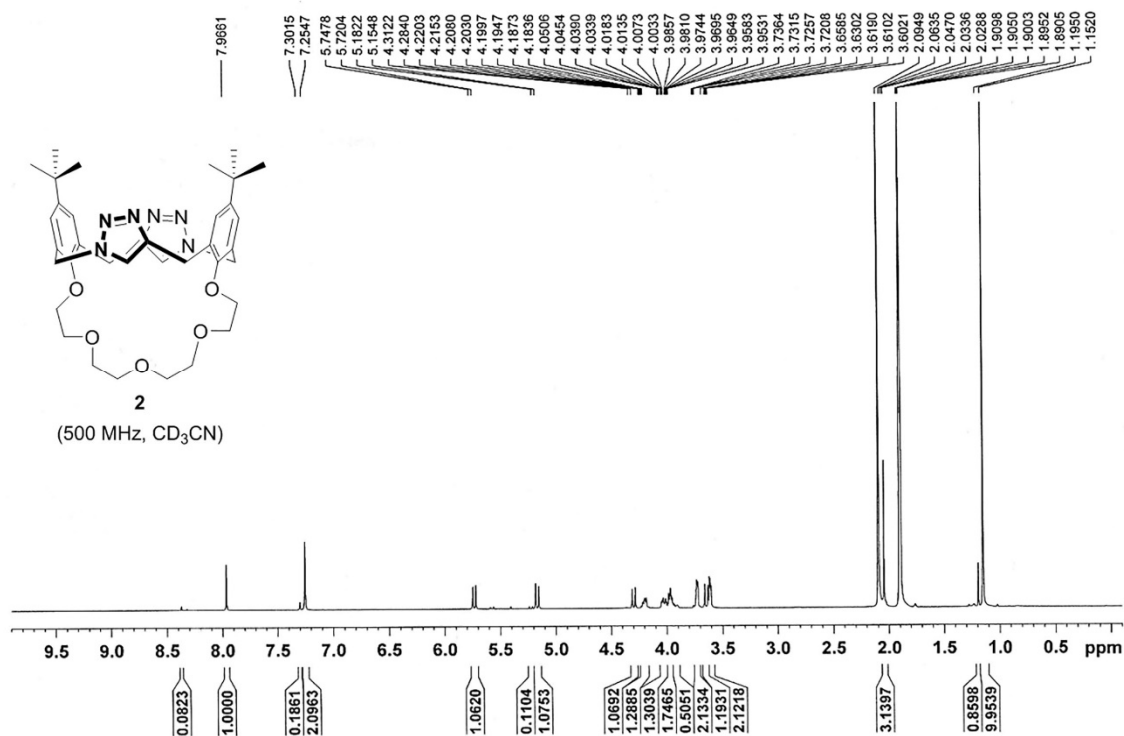


Figure S34. ¹H NMR spectrum of compound 2.

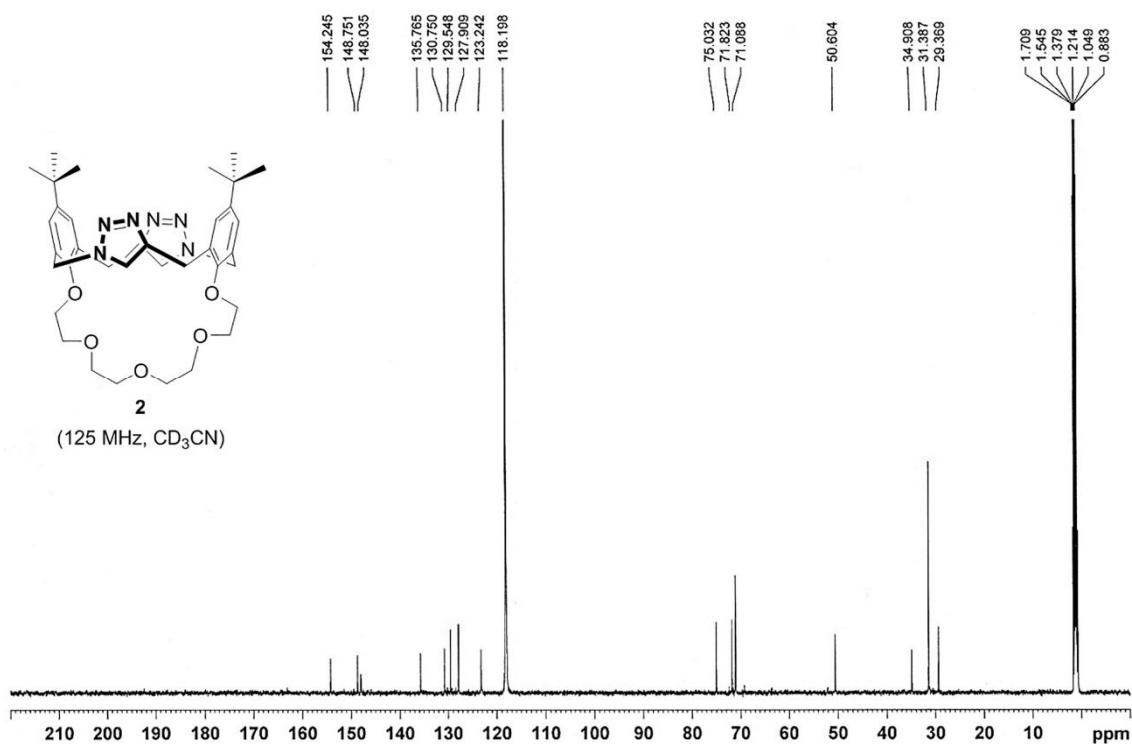


Figure S35. ¹³C NMR spectrum of compound 2.

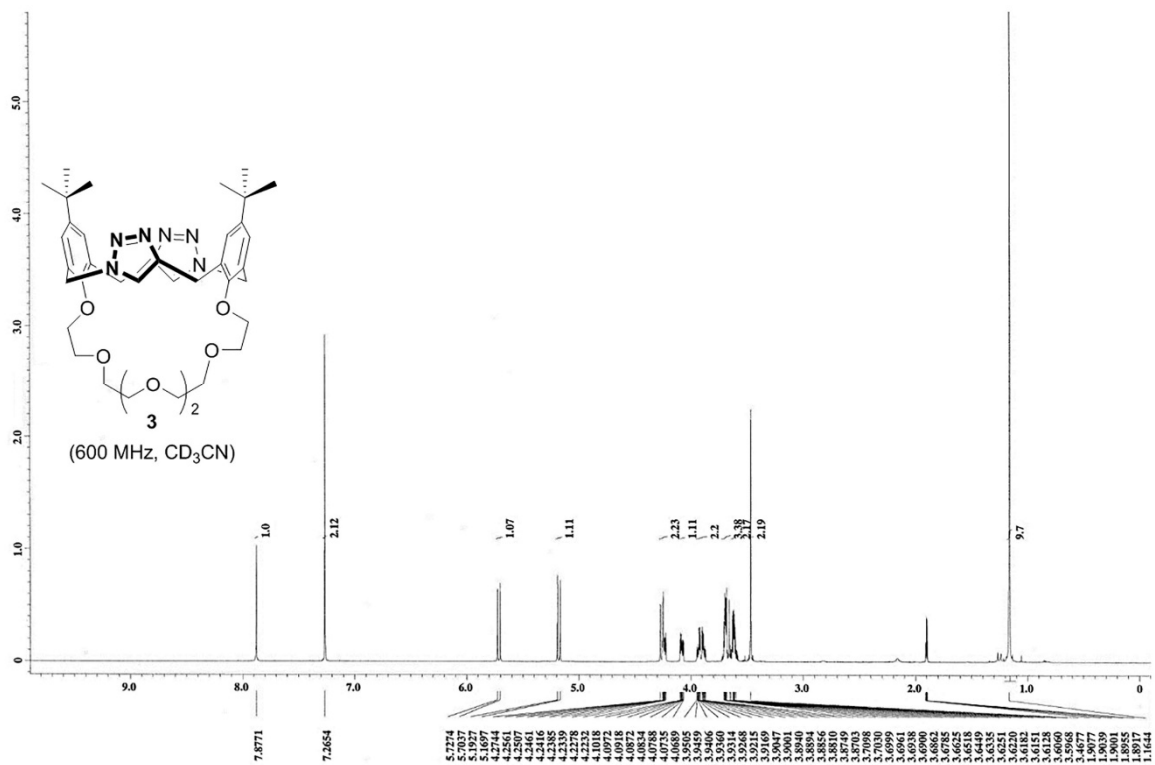


Figure S36. ¹H NMR spectrum of compound 3.

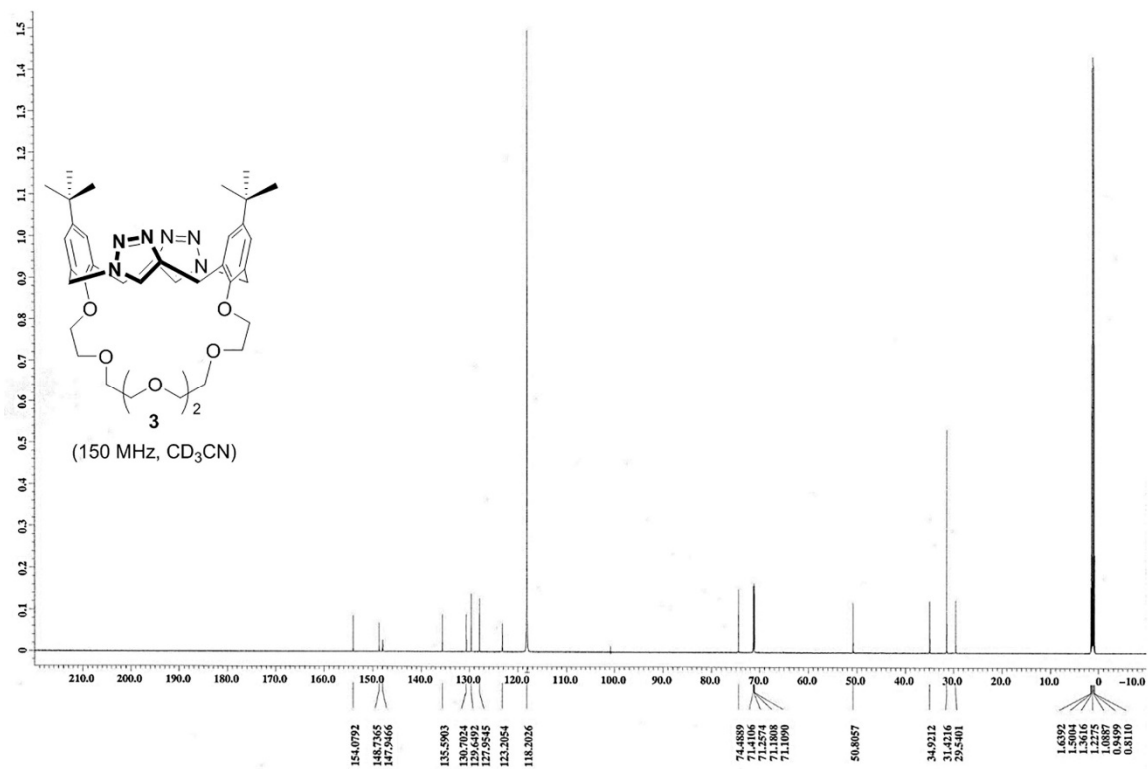


Figure S37. ¹³C NMR spectrum of compound 3.

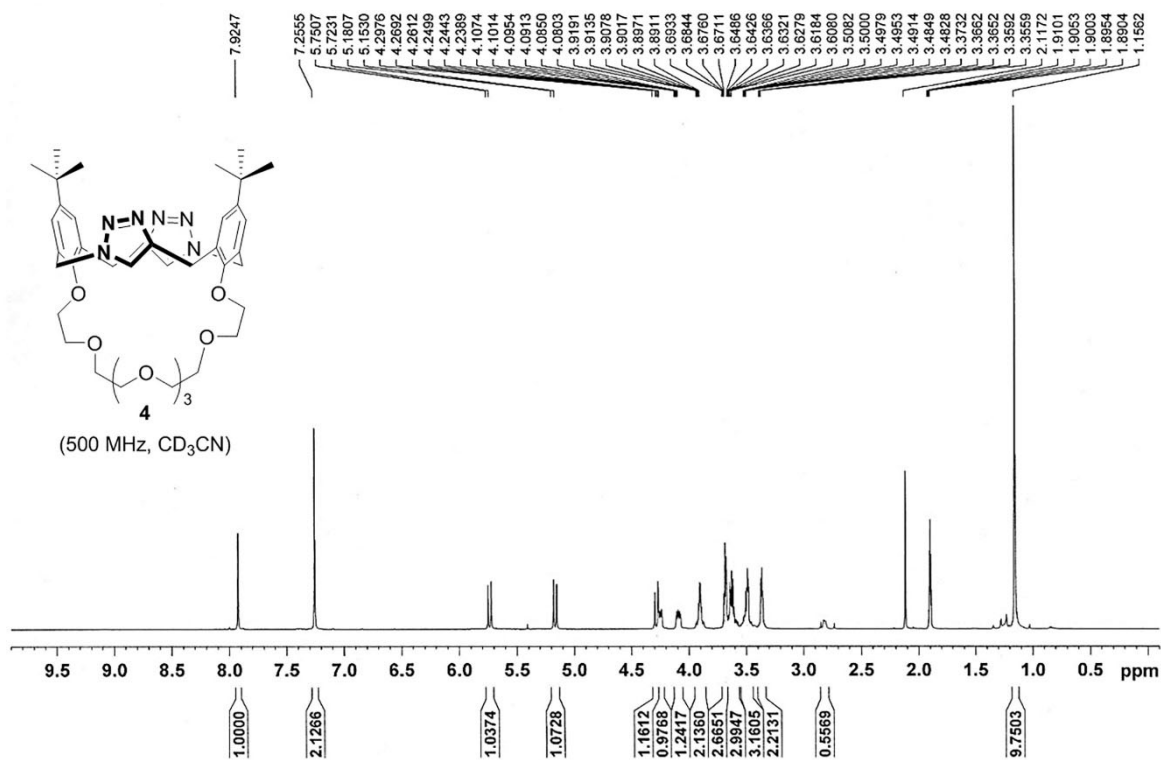


Figure S38. ¹H NMR spectrum of compound 4.

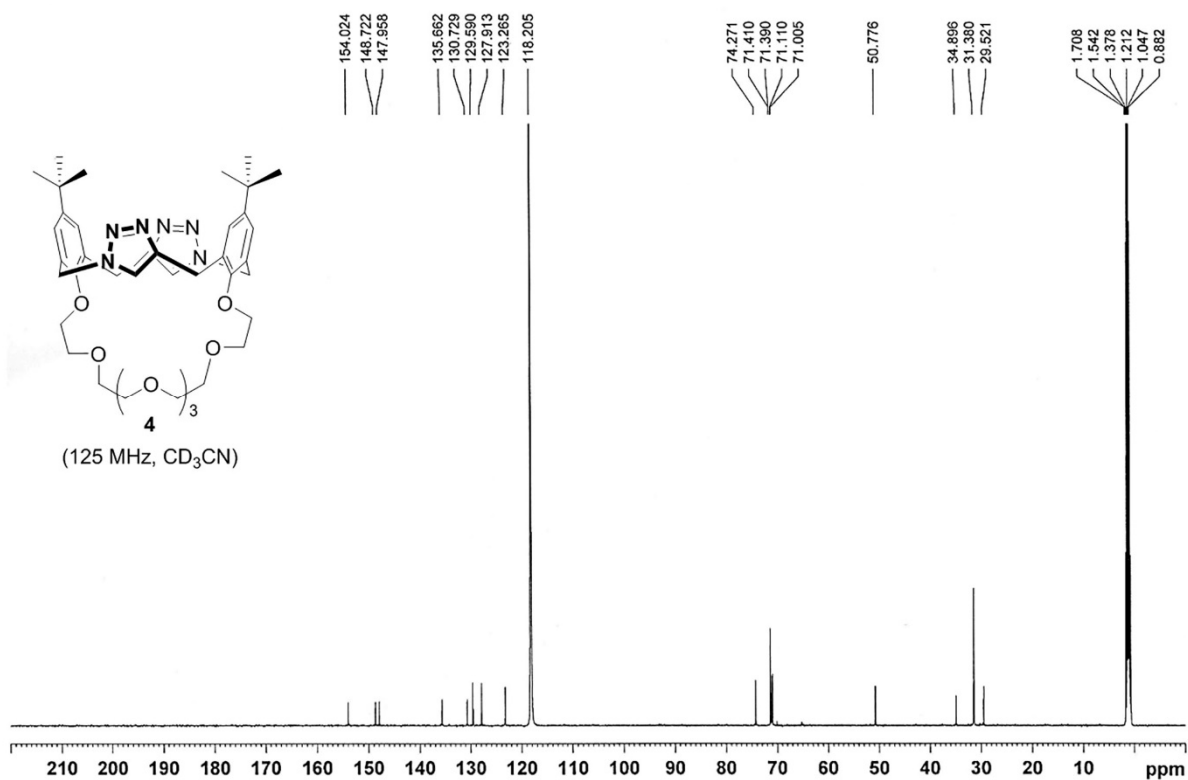


Figure S39. ¹³C NMR spectrum of compound 4.

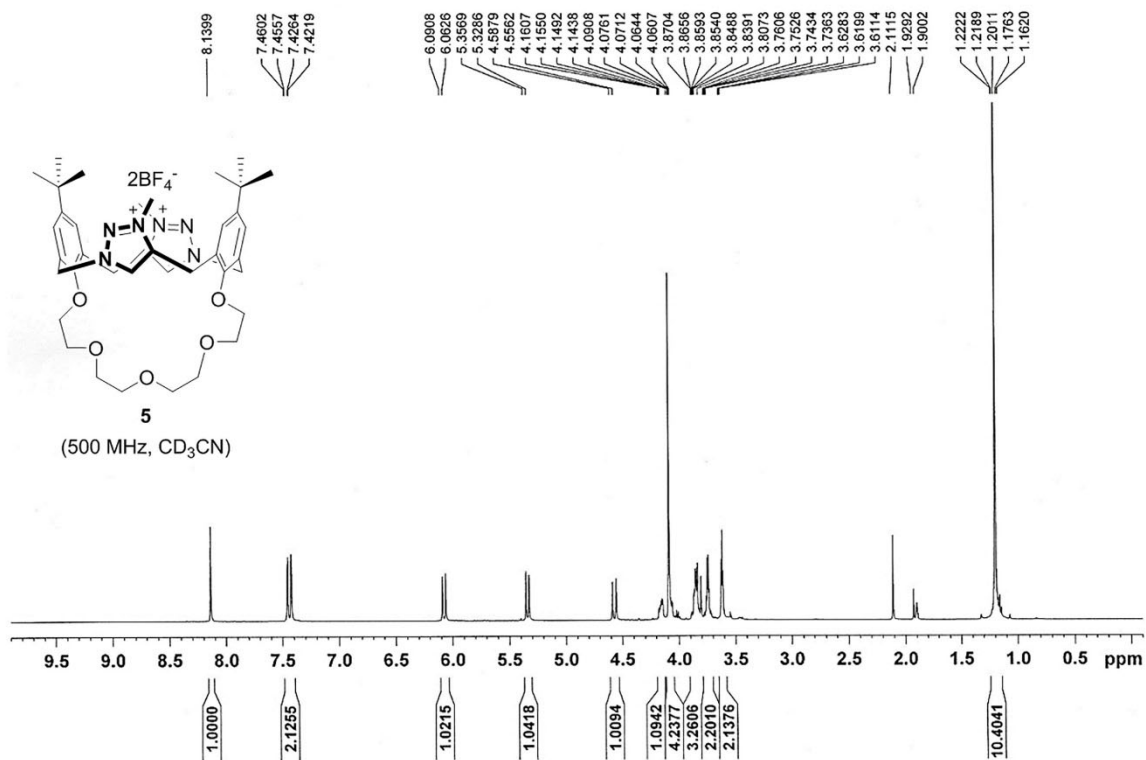


Figure S40. ¹H NMR spectrum of compound **5**.

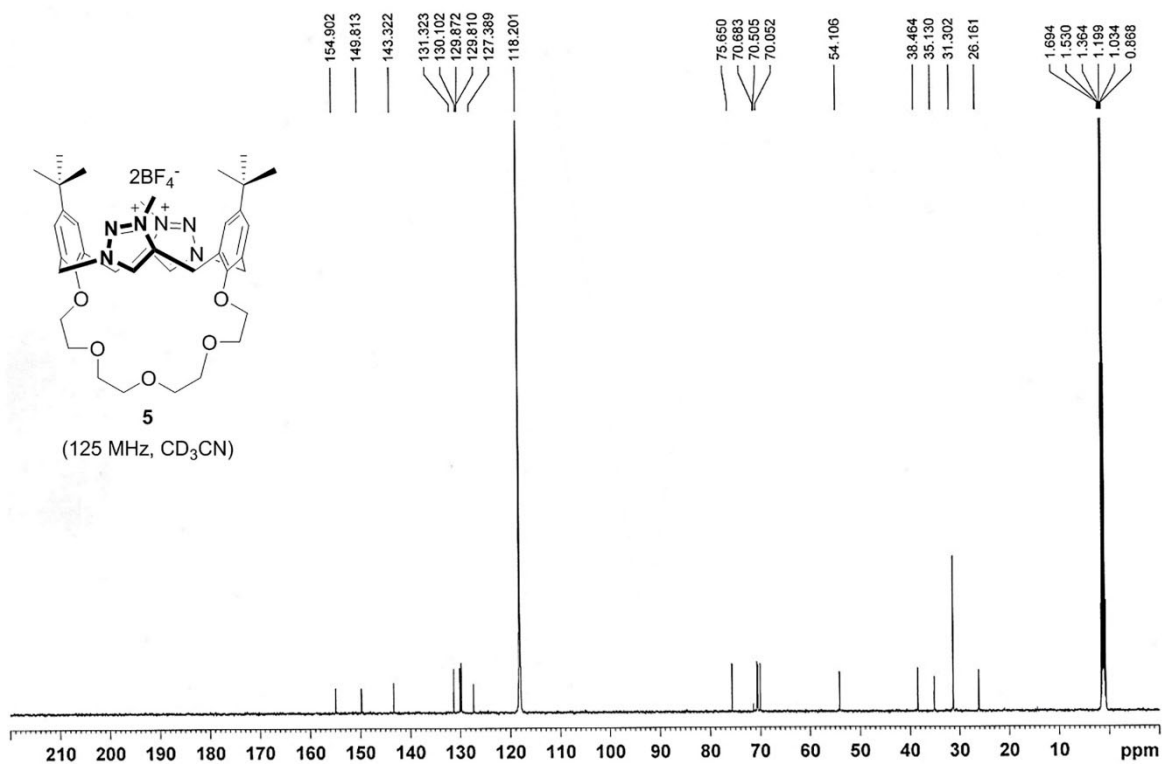


Figure S41. ¹³C NMR spectrum of compound **5**.

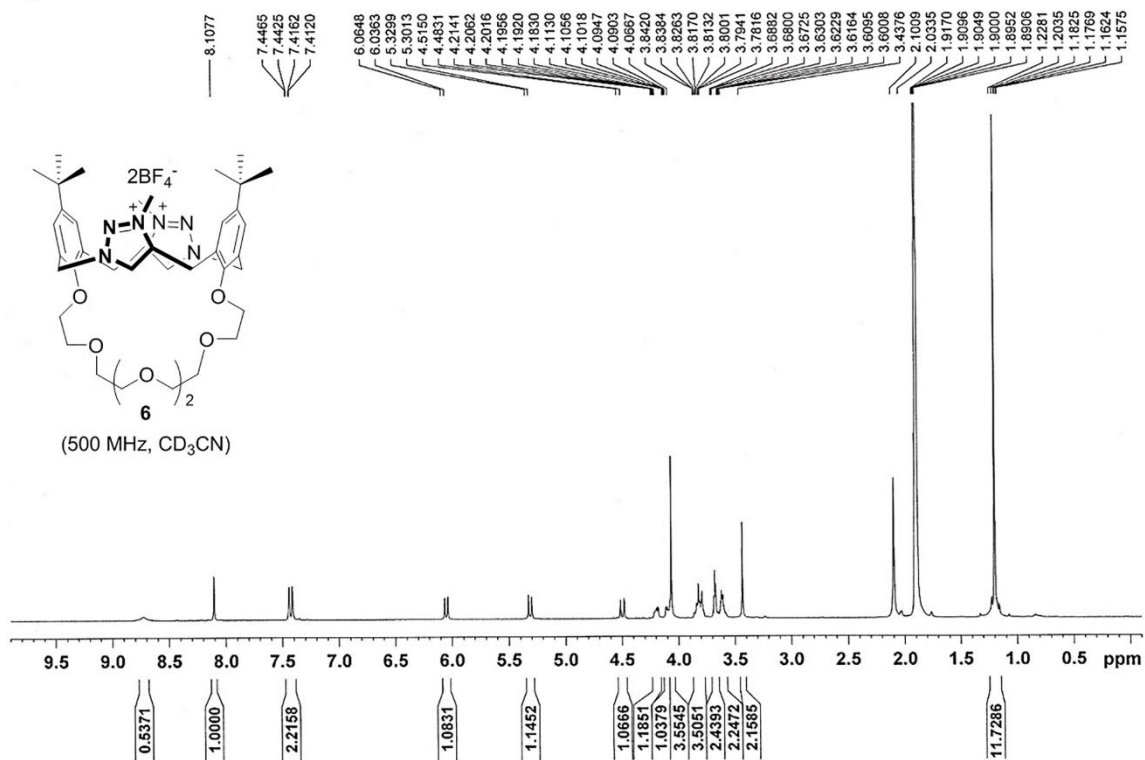


Figure S42. ¹H NMR spectrum of compound 6.

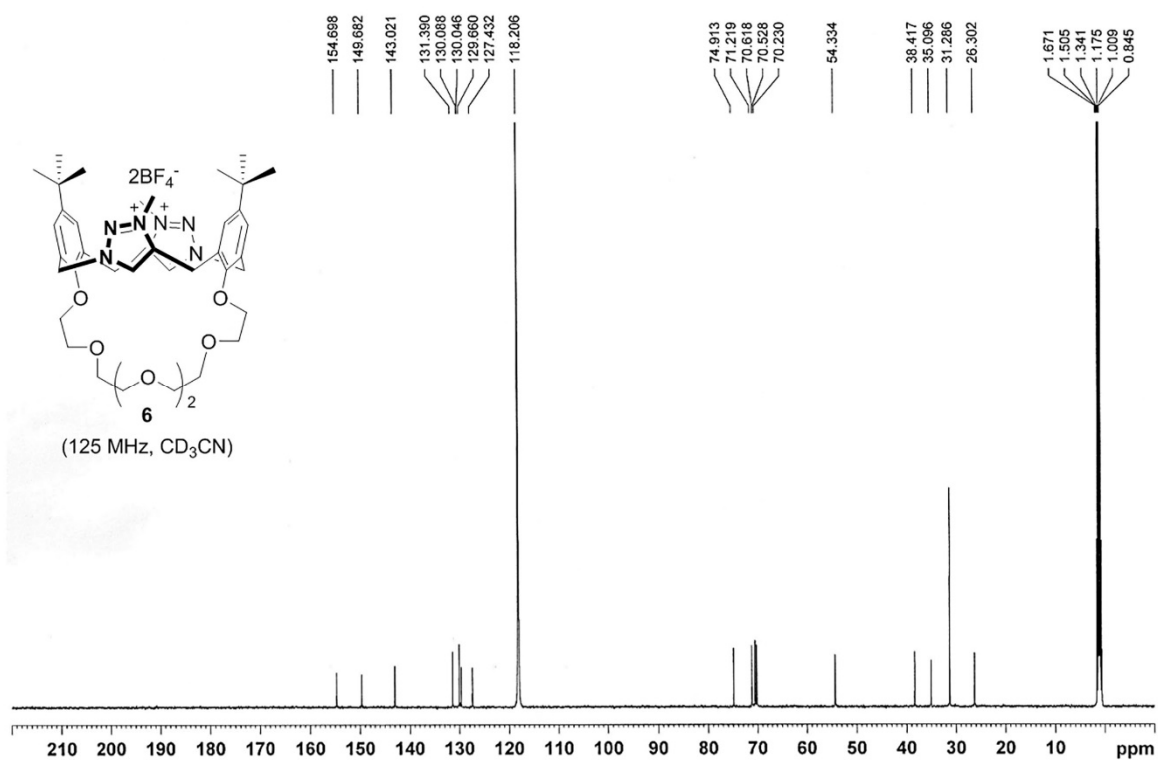


Figure S43. ¹³C NMR spectrum of compound 6.

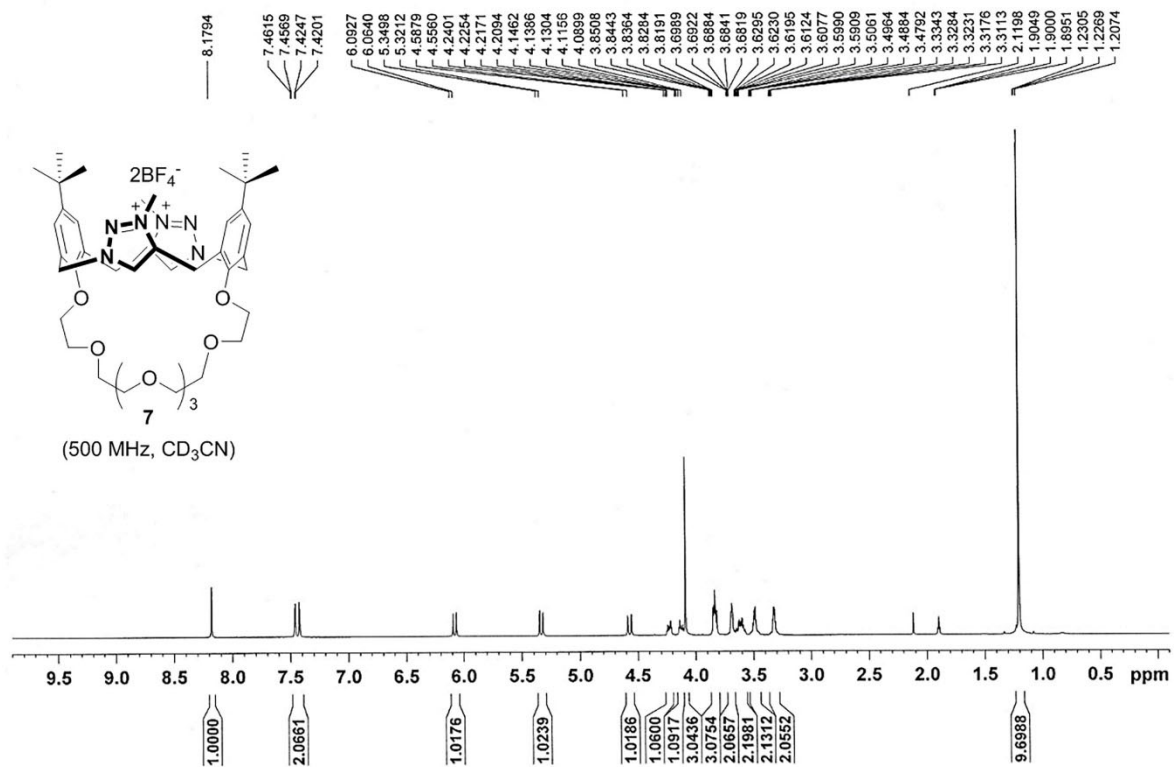


Figure S44. ¹H NMR spectrum of compound 7.

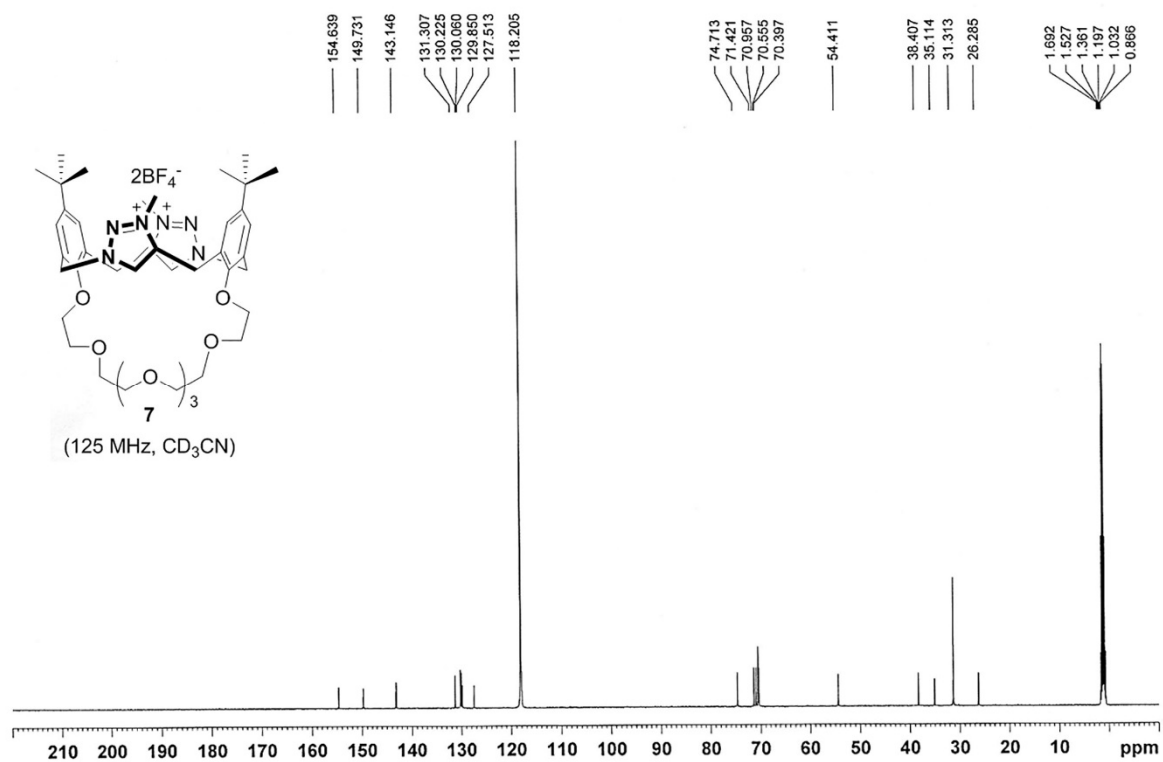


Figure S45. ¹³C NMR spectrum of compound 7.

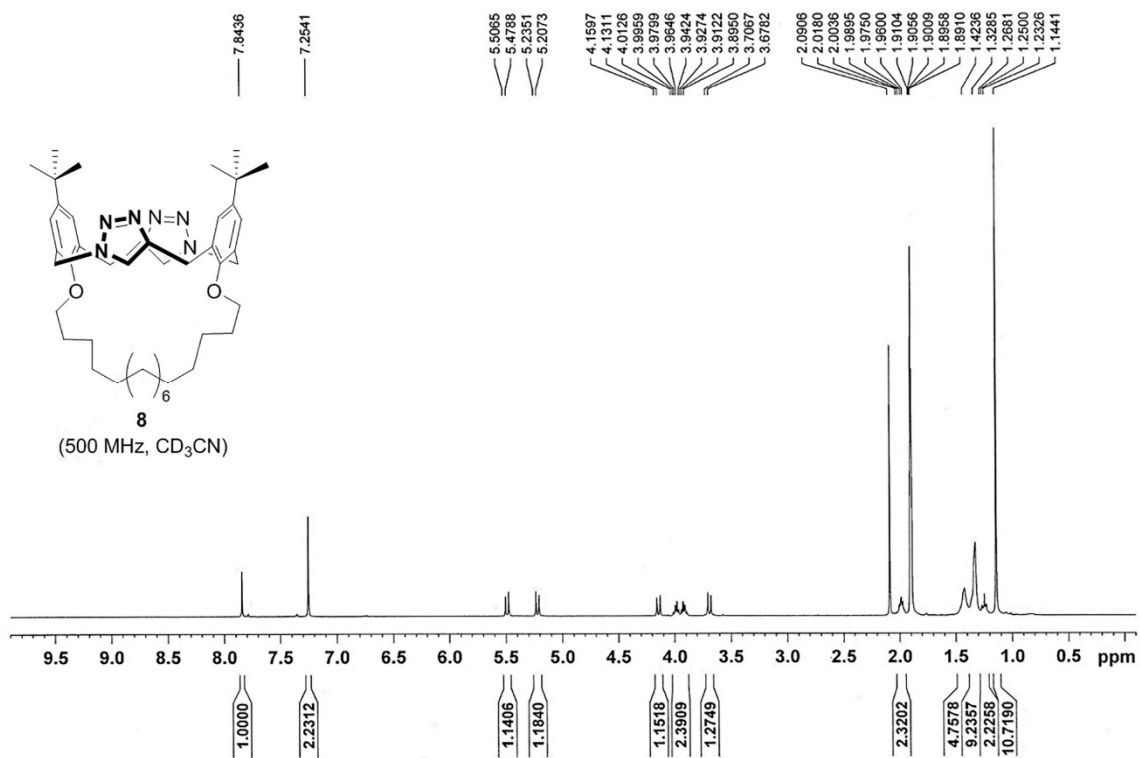


Figure S46. ¹H NMR spectrum of compound **8**.

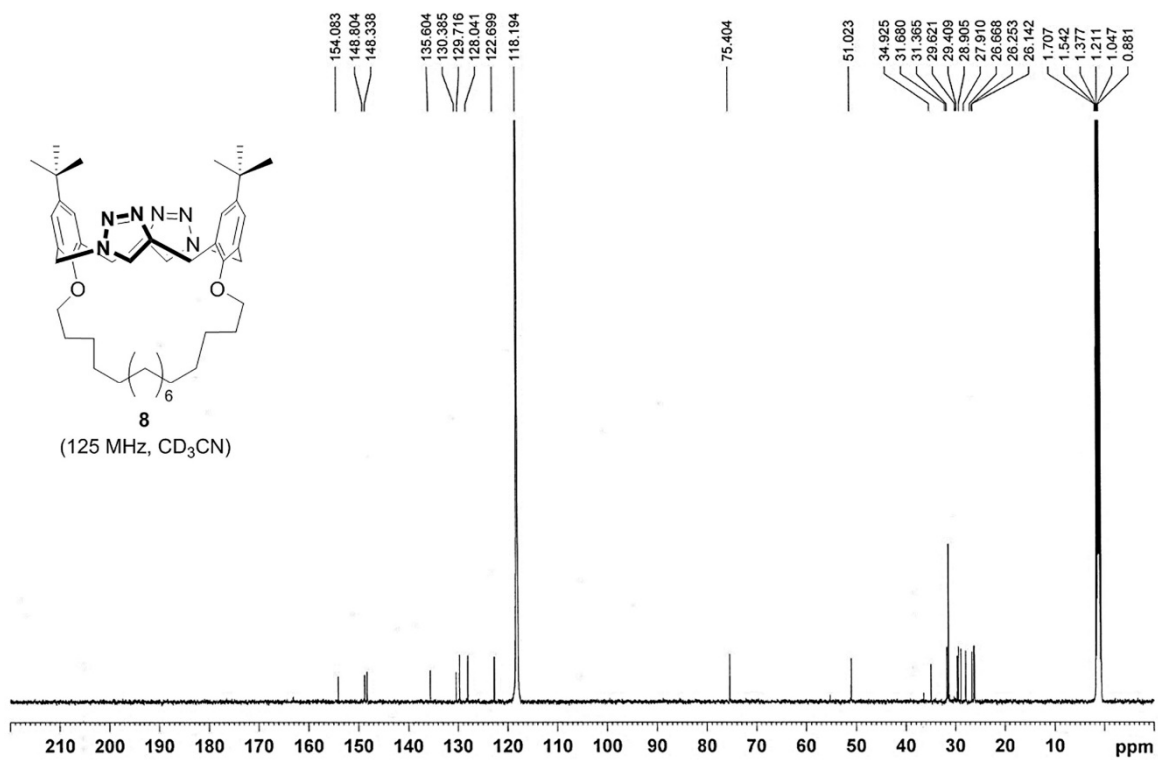


Figure S47. ¹³C NMR spectrum of compound **8**.

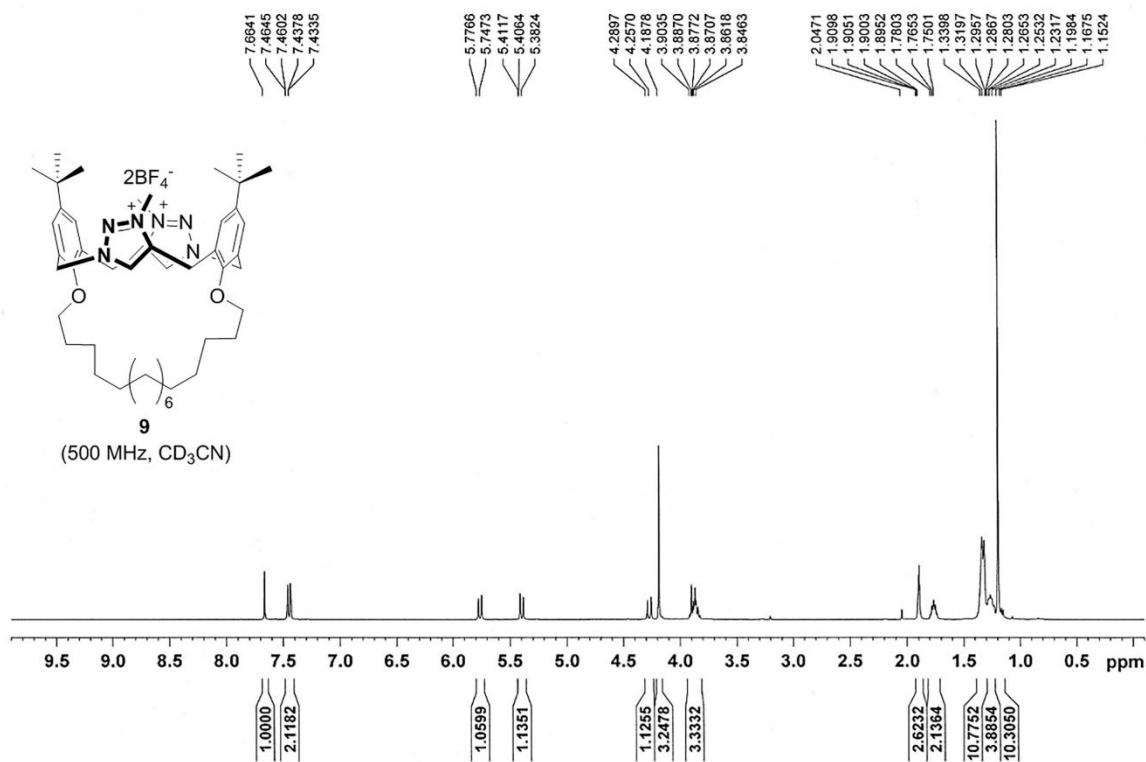


Figure S48. ¹H NMR spectrum of compound **9**.

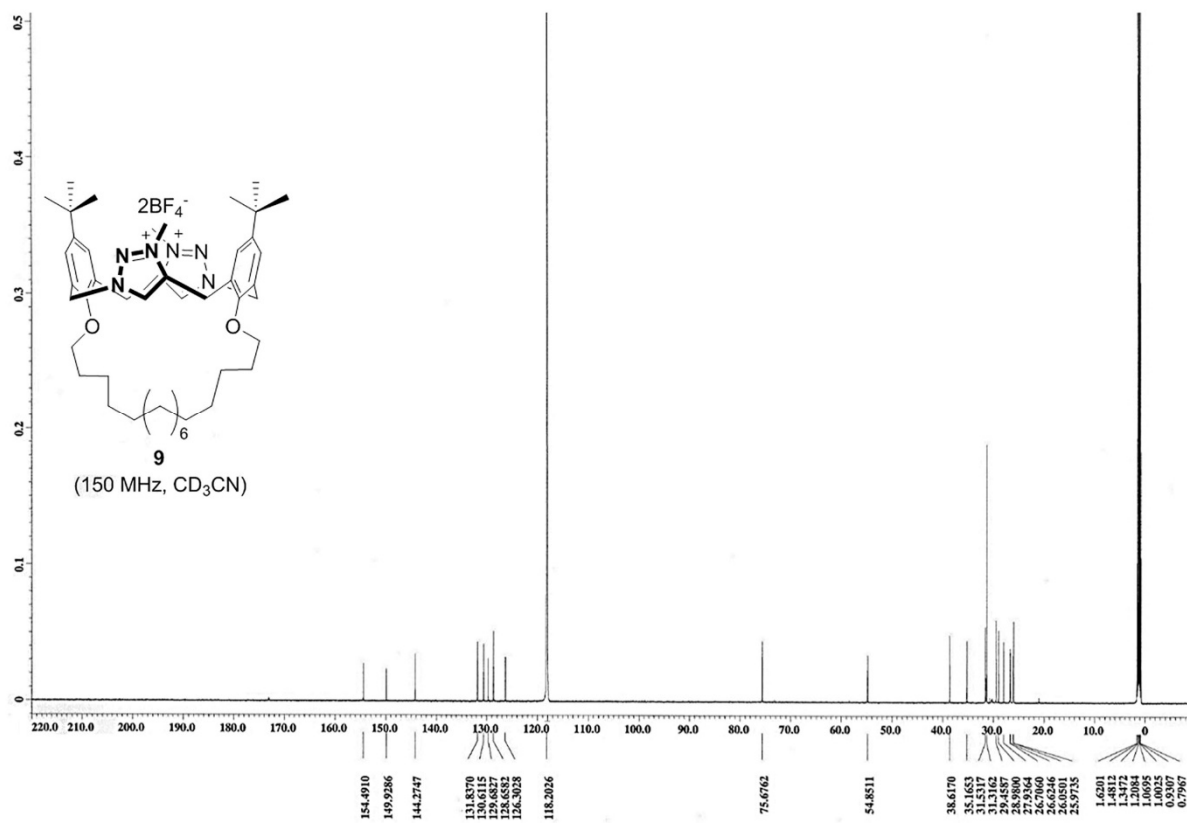


Figure S49. ¹³C NMR spectrum of compound **9**.

10. References

- S1 K. Muranaka, A. Sano, S. Ichikawa and A. Matsuda, *Bioorg. Med. Chem.*, 2008, **16**, 5862–5870.
- S2 (a) P. Van Der Sluis and A. L. Spek, *Acta Crystallogr., Sect. A: Fundam. Crystallogr.*, 1990, **46**, 194–201; (b) Commission on Charge, Spin and Momentum Densities, *Acta Crystallogr., Sect. A: Fundam. Crystallogr.*, 1990, **46**, FC1–FC4.
- S3 (a) T. Yanai, D. Tew and N. Handy, *Chem. Phys. Lett.*, 2004, **393**, 51–57; (b) W. J. Hehre, R. Ditchfield and J. A. Pople, *J. Chem. Phys.*, 1972, **56**, 2257–2261; (c) P. C. Hariharan and J. A. Pople, *Theor. Chem. Acc.*, 1973, **28**, 213–222; (d) M. M. Francl, W. J. Pietro, W. J. Hehre, J. S. Binkley, D. J. DeFrees, J. A. Pople and M. S. Gordon, *J. Chem. Phys.*, 1982, **77**, 3654–3665; (e) T. Clark, J. Chandrasekhar, G. W. Spitznagel and P. v. R. Schleyer, *J. Comp. Chem.*, 1983, **4**, 294–301.
- S4 J. Tomasi, B. Mennucci and R. Cammi, *Chem. Rev.*, 2005, **105**, 2999–3093.
- S5 Gaussian 16, Revision A.03, M. J. Frisch, G. W. Trucks, H. B. Schlegel, G. E. Scuseria, M. A. Robb, J. R. Cheeseman, G. Scalmani, V. Barone, G. A. Petersson, H. Nakatsuji, X. Li, M. Caricato, A. V. Marenich, J. Bloino, B. G. Janesko, R. Gomperts, B. Mennucci, H. P. Hratchian, J. V. Ortiz, A. F. Izmaylov, J. L. Sonnenberg, D. Williams-Young, F. Ding, F. Lipparini, F. Egidi, J. Goings, B. Peng, A. Petrone, T. Henderson, D. Ranasinghe, V. G. Zakrzewski, J. Gao, N. Rega, G. Zheng, W. Liang, M. Hada, M. Ehara, K. Toyota, R. Fukuda, J. Hasegawa, M. Ishida, T. Nakajima, Y. Honda, O. Kitao, H. Nakai, T. Vreven, K. Throssell, J. A. Montgomery, Jr., J. E. Peralta, F. Ogliaro, M. J. Bearpark, J. J. Heyd, E. N. Brothers, K. N. Kudin, V. N. Staroverov, T. A. Keith, R. Kobayashi, J. Normand, K. Raghavachari, A. P. Rendell, J. C. Burant, S. S. Iyengar, J. Tomasi, M. Cossi, J. M. Millam, M. Klene, C. Adamo, R. Cammi, J. W. Ochterski, R. L. Martin, K. Morokuma, O. Farkas, J. B. Foresman and D. J. Fox, Gaussian, Inc., Wallingford CT, 2016.
- S6 A. R. Allouche, *J. Comput. Chem.*, 2011, **32**, 174–182.
- S7 GaussView, Version 6, Roy Dennington, Todd A. Keith and John M. Millam, Semichem Inc., Shawnee Mission, KS, 2016.
- S8 (a) C. Adamo and V. Barone, *J. Chem. Phys.*, 1999, **110**, 6158–6169; (b) T. H. Dunning, *J. Chem. Phys.*, 1989, **90**, 1007–1023; (c) D. E. Woon and T. H. Dunning, *J. Chem. Phys.*, 1993, **98**, 1358–1371.
- S9 T. A. Keith and R. F. W. Bader, *Chem. Phys. Lett.*, 1993, **210**, 223–231.